Original Article

Biofpr
Biofuels Bioproducts & Biorefining

Feedstock planning and optimization of a sustainable distributed configuration biorefinery for biojet fuel production via ATJ process

Raul Mauricio Rivas-Interian, Eduardo Sanchez-Ramirez, Universidad de Guanajuato, Guanajuato, Mexico
Juan José Quiroz-Ramírez, Centro de Innovacion Aplicada en Tecnologias Competitivas (CIATEC), Leon, Mexico
Juan Gabriel Segovia-Hernandez, Universidad de Guanajuato, Guanajuato, Mexico

Received May 26 2022; Revised July 20 2022; Accepted August 16 2022;
View online December 2, 2022 at Wiley Online Library (wileyonlinelibrary.com);
DOI: 10.1002/bbb.2425; *Biofuels, Bioprod. Bioref.* 17:71–96 (2023)

Abstract: In recent years, the production and consumption of fossil jet fuel have increased as a consequence of a rise in the number of passengers and goods transported by air. Despite the low demand caused by the coronavirus 2019 pandemic, an increase in the services offered by the sector is expected again. In an economic context still dependent on scarce oil, this represents a problem. There is also a problem arising from the fuel's environmental impact throughout its life cycle. Given this, a promising solution is the use of biojet fuel as renewable aviation fuel. In a circular economy framework, the use of lignocellulosic biomass in the form of sugar-rich crop residues allows the production of alcohols necessary to obtain biojet fuel. The tools provided by process intensification also make it possible to design a sustainable process with low environmental impact and capable of achieving energy savings. The goal of this work was to design an intensified process to produce biojet fuel from Mexican lignocellulosic biomass, with alcohols as intermediates. The process was modeled following a sequence of pretreatment/hydrolysis/fermentation/purification for the biomass-ethanol process, and dehydration/oligomerization/hydrogenation/distillation for ethanol-biojet process under the concept of distributed configuration. To obtain a cleaner, greener, and cheaper process, the purification zone of ethanol was intensified by employing a vapor side stream distillation column and a dividing wall column. Once designed, the entire process was optimized by employing the stochastic method of differential evolution with a tabu list to minimize the total annual cost and with the Eco-indicator-99 to evaluate the sustainability of the process. The results show that savings of 5.56% and a reduction of 1.72% in Eco-indicator-99 were achieved with a vapor side stream column in comparison with conventional distillation. On the other hand, with a dividing wall column, savings of 5.02% and reductions of 2.92% in Eco-indicator-99 were achieved. This process is capable of meeting a demand greater than 266 million liters of biojet fuel per year. However, the calculated

Correspondence to: Juan Gabriel Segovia-Hernandez, Universidad de Guanajuato, Noria Alta s/n, Guanajuato 36050, Mexico. E-mail: gsegovia@ugto.mx

sale price indicates that this biojet fuel still does not compete with conventional jet fuel produced in Mexico. © 2022 Society of Chemical Industry and John Wiley & Sons, Ltd.

Supporting information may be found in the online version of this article.

Key words: biojet fuel; stochastic optimization; process intensification; lignocellulosic biomass

Introduction

The production and consumption of fossil fuels have been engines of the world economy for a long time. However, dependence on oil is increasingly evident due to its scarcity and, consequently, elevated prices. On the other hand, the presence of pollutant emissions involved in petroleum-based processes and throughout the fuel value chain have reached alarming levels. Minimizing the dependence on fossil fuels and reducing the generation of greenhouse gases (GHGs) caused by their production and consumption represent a challenge for the industry. The use of biofuels is capable of counteracting the negative effects of conventional fuels on the economy and environment. Consequently, the design of biorefineries is a necessary task on the path to the sustainability promoted by biofuels. Regarding the fuels value chain, the concept of the circular economy has emerged as a response to the linear economy adopted in the past. The circular economy aims to replace fossil resources gradually with renewable resources to satisfy the demand of the worldwide population for energy and chemicals in sustainable ways. It achieves this by optimizing the yields from virgin resources through the manufacturing of more reusable products, and by reducing the generation of waste.[1] Biomass is very important in a circular economy in terms of an adequate use of organic waste that allows the generation of chemical products and biofuels. To establish a circular economy, the practical implications of the use of biomass need to be appreciated by stakeholders throughout the value chain, from product design to waste management.[2]

In recent years, the growth of the air traffic sector has been the driving force of global transport and it has played an important role in promoting social and business contacts worldwide. During 2017, more than 4.1 billion passengers and 539 million metric tons were transported, which represents about 35% of global trade by value. The number of passengers is expected to double by 2036, increasing jet fuel consumption.[3,4] However, this forecast is continuously changing as a consequence of the pandemics caused by severe acute respiratory syndrome coronavirus 2 (SARS-CoV-2). In this regard, the activity of the air traffic sector was reduced between 10% and 15% in April and May 2020, to about the levels reached in 2019. In November 2020, a total of 16.4 million flights were counted against 38.9 million flights in November 2019.[5]

Despite the global situation created by coronavirus 2019 (COVID-19), slow-growing demand for jet fuel is expected as a result of the global economic recovery. This occurs in a context where the price of fossil fuels rises while petroleum is increasingly scarce. The production and consumption of jet fuel are causes of the continuous increase in greenhouse gasses (GHGs), which contribute to global warming. The aviation sector is one of the faster growing GHG sources, at a rate of 5.7% per year (6), and it is responsible for 1.9% of such emissions (7).

Mainly motivated by the increase in jet fuel prices and its inherent environmental impact, the production of biomass-based alternative fuels in a framework of circular economy emerges as a promising solution to the dependence of many countries on fossil fuels and to the effects of global warming. In this context, one of the liquid fuels that has gained attention as a substitute for conventional jet fuel is biojet fuel.[9]

Different routes of production for biojet fuel offer various advantages and disadvantages. Oil-based biojet fuel has been produced widely and several low-cost technologies have been tested successfully. The most popular are hydroprocessing of esters and fatty acids (HEFA), catalytic hydrothermolysis (CH), and hydroprocessing to depolymerized cellulosic jet (HDCJ).[4,10–12] However, the raw material for the oil path has proven not to be entirely sustainable. In this regard, there is a shortage of arable land for oilseeds and, if available, they compete with land for food crops. In the particular case of *Jatropha curcas* crops, although they are capable of growing in varying agroclimatic conditions, they are accompanied by variations in important parameters such as seed yield, oil content, and nutrient requirements, which critically affect the economic viability of plantations.[13,14] This path also contradicts the principles of the circular economy because oil crops do not arise as a by-product but as a parent feedstock.

A route that has not been explored as much as the oil route is that of alcohols. Alcohols can be produced from lignocellulosic biomass, which is considered to be the main promising renewable resource, as it is largely available around the world and its use avoids the food versus fuel conflict

related to the use of edible crops. The full recycling and reuse of agro-industrial lignocellulosic waste contributes to the circular economy because this renewable resource can be used repeatedly to generate valuable and marketable products, replacing the exhaustible fossil-based resources.[1]

Through the pretreatment, saccharification, and fermentation processes, agro-industrial lignocellulosic wastes can be converted into short- and long-chain alcohols. Particularly interesting is the upgrading of lignocellulose into bioethanol. As a green and cheap alternative to petrochemical fuels, being the most commonly used liquid biofuel, bioethanol is receiving much attention due to the development of technology conversion, which improves its platform.[1] Bioject fuel can be obtained easily from bioethonical through dehydration to produce ethylene, oligomerization, and hydrogenation. This upgrade is known as the alcohol-to-jet process (ATJ).

The whole conversion process from lignocellulosic biomass to biojet fuel through alcohols presents several areas of opportunity to reduce capital and operational costs and environmental impact. One of the strategies to obtain a process that meets the sustainability requirements comes from process intensification, which refers to a set of tools capable of achieving dramatic improvements in manufacturing and processing by substantially decreasing equipment size, waste production, and energy consumption. This leads to smaller, cleaner, and more energy-efficient processes.[15]

This process also faces challenges. A critical step relates to the raw material, its seasonal nature, and annual variability in the biomass supply. Most biomass sources are vegetal material, which needs to be planted, cultivated, and harvested through a growth cycle. It has also been reported that the time and frequency of the harvest can affect the yields of energy crops, so it would be necessary to plan and schedule the production carefully to guarantee the quantity and quality of the biomass supply.[16]

To date, no research addressing the design and optimization of biojet fuel production from lignocellulosic alcohols under sustainability criteria has been published. This work aims to present an optimized process design to produce biojet fuel from ethanol through the ATJ process in an economical and environmentally friendly way, taking Mexican agro-industrial lignocellulosic biomass as feedstock to accomplish the goals of the circular economy.

General description of the process

The overall process of biojet fuel production with alcohols as intermediates requires the processing of lignocellulosic biomass to produce such alcohols. The general scheme for the production of alcohols from lignocellulosic agro-industrial waste involves four steps (Fig. 1): the pretreatment of biomass, to break down cell walls into cellulose and hemicellulose, and to remove lignin; hydrolysis (or saccharification) of biomass; the fermentation of produced monosaccharides (pentoses and hexoses) to alcohols by the action of yeasts, bacteria, or other appropriate organisms; and the purification of the alcohol.[17]

Once the alcohols have been obtained, they are sent to the ATJ process to be upgraded to biojet fuel. The core of the ATJ process is a concept developed to bridge the gap between alcohols that can easily be produced from renewable resources and the high-quality hydrocarbon fuels needed in aircraft turbines. This process is based on three catalytic reactions: dehydration of alcohol, oligomerization of olefins, and hydrogenation, followed by the separation of the synthetic paraffin product in the jet fuel range, as shown in Fig. 2. The residual products of the process are used as gasoline and diesel.[19] Short-chain alcohols such as ethanol, *n*-butanol, and isobutanol have been of particular interest as raw materials and can be produced from lignocellulosic biomass or waste. The first renewable aviation fuel approved by ASTM D7566 was biojet fuel derived from isobutanol, allowing mixtures

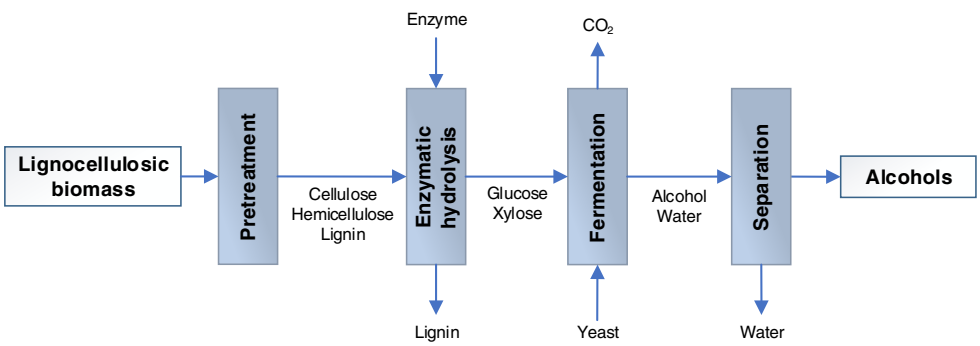

Figure 1. Conversion process from biomass to ethanol.[17,18]

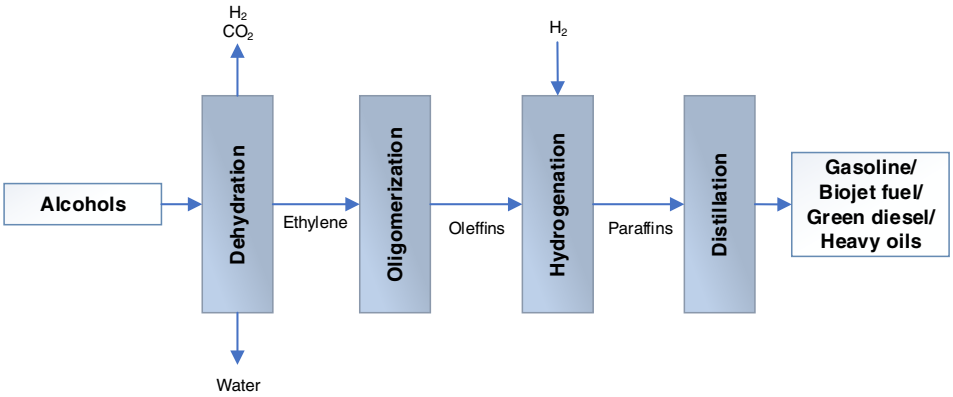

Figure 2. Alcohol-to-jet process.

of up to 30% with conventional jet fuel. On the other hand, ethanol has recently been approved as a raw material allowing the biojet fuel produced from it to be mixed with conventional jet fuel in mixtures containing up to 50% renewable fuel.[20]

The production of lignocellulosic ethanol is still unprofitable, and it is difficult to predict when its cost will be reduced to the level of first-generation ethanol, but progress can be made by considering its production in the framework of an integrated biorefinery to obtain naphtha, gasoline, diesel, and heavy oils among other value-added products. However, the starting point can be any alcohol, ethanol, butanol, etc. In this work, ethanol was selected as the starting alcohol due to its technological maturity in comparison with other bioalcohols. In addition to technological maturity, effluents from the fermentation of this alcohol have a higher concentration of ethanol than other bioalcohols, which will eventually be reflected in higher jetfuel production.[10,21,22] In the case of ethanol, its maximum use in most gasoline-powered vehicles as an additive is in mixtures of 10% to 15%, which creates a barrier to its market penetration as an additive for gasoline. This, coupled with advances in production efficiency and diversification of the raw material, would result in excess production of ethanol at competitive prices. It would also be available to produce a wide range of platform fuels and chemicals. Its transformation into biojet fuel therefore presents an area of opportunity to achieve greater profitability from alcohol.[10,20] Another area of opportunity concerns the purification of ethanol from fermentation broths. Extractive distillation for ethanol presents relatively high costs but, despite this disadvantage, it remains the main choice in the case of large-scale ethanol production. Ethanol purification has been studied widely, and high costs and elevated energy consumption have been demonstrated. For this reason, a first approach on the path to sustainability is its intensification. By intensifying this process, economic and environmental improvements can be achieved and a safer, energy-efficient, cleaner, cheaper, and greener process can be obtained as various authors have reported.[23–25]

A number of studies focusing on the design of the entire biorefinery have also appeared in the literature. Approaches to biorefinery design can be categorized into two types (Ng and Maravelias).[26,27] In the centralized configuration biomass is transported directly to the biorefinery and pretreated on site. Decisions typically considered in these models include biomass selection and allocation at farms, and technology selection and capacity planning at the biorefinery. The objective is the maximization of profit, or minimization of cost, of the entire biofuel. On the other hand, the concept of a collection facility or regional biomass processing depot has been introduced to improve the handling efficiency of biomass and to reduce transportation cost and CO_2 emissions. Biomass is pretreated and/or densified to a higher density intermediate for ease of transportation and storage. It can be shipped directly to the biorefinery if this leads to economic or environmental benefits. For the distributed configuration, additional decisions related to the depot such as facility location, technology selection, and capacity planning are considered. Bowling *et al.*[26] and Ng and Maravelias[27,28] showed that the distributed configuration has lower costs than the centralized configuration.

Sustainable, green, and efficient processes are among the top priorities required in the chemical industry to address the grand challenges of resource depletion, energy consumption, and climate change. The identification, design, and development of appropriate processes are therefore important for the industry to remain competitive, and more sustainable and efficient processes should be achieved as a primary objective (Garcia-Serna[29]). Consequently, the design of a sustainable biorefinery will result in a cleaner, more energy-efficient operation. The complexity of these

Table 1. Feedstock composition in dry basis (%wt).[35]

Feedstock	Cellulose	Hemicellulose	Lignin	Ash	Moisture
Sugarcane bagasse	44	31	23	2.0	50
Corn stover	39	33	26	2.0	20

objectives necessitates the use of an integrated approach, which addresses the interactions among the different unit operations and technologies within the process. It is also important to reconcile the often-competing objectives dictated by economics and the environment through the generation of systematized methodologies (Foo and El-Halwagi[30]). The contribution of this paper is to generate a systematized methodology to find optimal designs of biorefineries where the interactions between the different indicators are balanced to obtain optimal configurations.

Taking into account these considerations regarding the use of lignocellulosic agro-industrial waste and process intensification to decrease total costs and environmental impact, the process is designed to obtain biojet fuel more sustainably, within the framework of the circular economy. As far as the authors are aware, no study on the concept of sustainability is available in the literature on the production of bio jet fuel.

Case study

A feasible scenario for bioturbosine production in Mexico is to cover the demand of at least 5.5% of conventional biojet (31). Covering 5.5% of total demand represents a biojet production of 258 million liters. The production of biojet fuel from ethanol involves a series of steps that involve the production of ethanol from lignocellulosic biomass. The availability of biomass limits the whole process, making it necessary to consider the seasonality of the crops and, therefore, of their waste when planning the feedstock. To satisfy the demand for biojet fuel, more than one feedstock has to be considered. To leverage the number of available pretreatment technologies and their ability to break biomass, more than one pretreatment is necessary. The planning of the feedstock and the diverse combination of feedstocks and pretreatments make it possible to organize the process within a superstructure scheme.

Feedstock selection

Based on the information provided by the Servicio de Información Agroalimentaria y Pesquera and by Mexican Ministry of Agriculture and Rural Development (SAGARPA),[32] sugarcane bagasse and corn stover were selected as feedstocks, as they were the most abundant biomasses in Mexico during 2018. Sugarcane bagasse and corn stover can also be potential substrates for ethanol production because they have high sugar content and are renewable, cheap, and readily available feedstocks.[33,34] The process was developed to obtain the necessary sugars from these biomasses to produce ethanol. Table 1 shows the composition of cellulose, hemicellulose, and lignin on a dry basis, as well as the percentage of moisture of the biomasses in Mexico.

Pretreatment selection

Possible pretreatments were selected based on the evaluation made by Conde-Mejía *et al.*[36] taking as selection criteria the cost of energy consumed in the operation per tonne of dry biomass and the cost of energy per gallon of bioethanol produced reported in their work. In this respect, the most economical alternatives were pretreatment by steam explosion and dilute sulfuric acid. In addition to the operating costs, another important factor to take into account in the pretreatment selection was the tendency for degradation to form products that inhibit fermentation. Under certain conditions of residence time, temperature, and concentration of sulfuric acid the formation of inhibitors is negligible. Previous research includes the range of conditions in which this can be accomplished. They are reported in Table S2 of the Appendix S1. The literature also reports other effective pretreatments that do not generate inhibitors. Ammonia fiber explosion (AFEX) pretreatment is one of them. However, the recovery of ammonia from the process and the requirements for a new amount of ammonia increase the capital and operating costs for AFEX[37] and, according to Conde-Mejía *et al.*[36] its energy cost is two to three times more than those for steam explosion and dilute sulfuric acid.

Feedstock planning design

To take into account the availability of crops and, therefore, of agricultural waste, planning was designed, the variables of which were part of the subsequent optimization process. The design was distributed as shown in Fig. 3 for each month of the year.

In Fig. 3, X represents the amount of cellulosic sugar obtained from sugarcane bagasse, Y represents the fraction of sugars from sugarcane bagasse pretreated by steam explosion, and Z represents the fraction of sugars from corn stover pretreated by steam explosion.

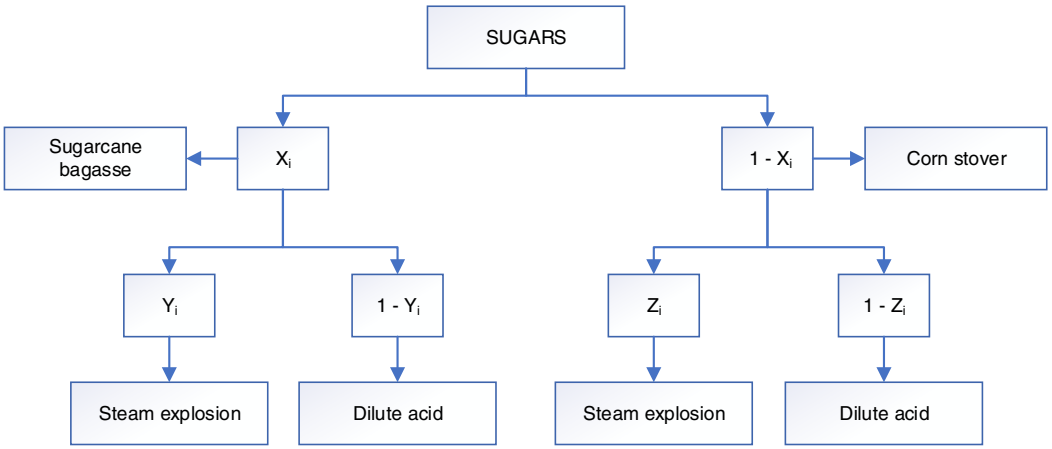

Figure 3. Definition of planning variables.

Process modeling

Ethanol is not a single-use intermediate, but it can be employed as a building block for fuels and various chemicals,[38] ethanol can be competitive in the market and be sold when required, according to market needs, and avoid low profitability in the process when the demand for biojet fuel is low or there is no demand. For this reason, the whole process was modeled in two parts. The first part involved obtaining ethanol from lignocellulosic biomass. The second part concerned the production of biojet fuel from ethanol. In a modular manufacturing scheme, this allows the ethanol plant to be located near to harvest sites and the biojet plant to be located near to the airports, thus reducing supply chain costs, increasing the flexibility of the whole process, and allowing the production network to react to dynamic supply and demand developments.[39-42]

Ethanol process design

The process of obtaining ethanol from lignocellulosic biomass was designed under a superstructure scheme that took into account the two biomasses and the two pretreatments previously selected.

Reactor modeling was performed by adjusting experimental data to polynomial equations. This was done in Minitab 19 by employing the 'fit regression model' tool. According to what is reported in the literature, it was decided to consider the same type of biomass (sugarcane and corn) for all the case studies. The intention is to make a direct comparison between the case studies considering dilute acid and steam explosion as pretreatment mechanisms. In the case of fermentation, this homogeneity in the data was not necessary, due to the fermenters processing liquid streams with glucose independently of the solid biomass type, unlike previous reaction steps where experimental data did depend on the type of biomass.

Reactors in this process were modeled in Microsoft Excel, while the purification of ethanol was modeled in Aspen Plus 8.8. Both were connected through macros from Visual Basic. Model equations for reaction steps are described below. Details about the polynomial coefficients and their validity intervals are shown in the supplementary material. For the pretreatment section, the data and their limits were carefully selected taking into account the range from which the formation of inhibitors begins (Table S2 in the Appendix S1).

The following assumptions were made for reaction modeling:

a. The five and six carbon sugars are grouped into a single fraction as hemicellulose and cellulose, respectively.
b. Entire fractions of cellulose and hemicellulose are comprised by glucan and xylan, respectively.
c. The lignin remains as an inert material.
d. The amount of inhibitors produced during the pretreatment is negligible in the range of conditions from experimental data.
e. The enzyme employed in the enzymatic hydrolysis only breaks the glucan chain into glucose. Furthermore, xylan hydrolysis does not occur.
f. The yeast microorganism (*S. cerevisiae*) is only able to ferment glucose sugar into ethanol and carbon dioxide.

Pretreatment modeling The following prehydrolysis reactions were carried out:[43]

$$(Glucan)_n + nH_2O \rightarrow nGlucose \quad (1)$$

Table 2. Polynomial regression coefficients for pretreatment modeling.

	Steam explosion				Dilute sulfuric acid			
	Sugarcane bagasse		Corn Stover		Sugarcane bagasse		Corn Stover	
	Glucan	Xylan	Glucan	Xylan	Glucan	Xylan	Glucan	Xylan
A	5.653E–03	3.434E–02	1.295E–02	2.109E–02	1.246E–02	3.040E–02	4.687E–03	–7.490E–03
B	2.943E–02	–2.198E–02	2.590E–03	–6.500E–03	–4.250E–02	–4.315E–03	1.097E–01	5.687E–01
C					–3.180E–01	–1.430E+00	2.000E–02	–2.900E+00
D		–1.670E–04	–4.231E–05	–9.310E–05	–4.010E–05	–2.760E–04		
E		1.790E–04	6.700E–06	1.077E–04				–3.769E–02
F					3.000E–03	3.100E–01		–3.260E–01
G	–1.720E–04	–2.000E–06	–2.550E–05	–3.260E–05	2.480E–04		–5.490E–04	–1.200E–04
H					1.810E–03	7.100E–03	3.200E–04	1.216E–02
I					8.570E–02			3.826E–02
J					–5.130E–04			
K						–1.600E–03		
L						6.300E–07		
Coefficient of determination (R^2)								
	99.86%	98.34%	99.99%	99.54%	99.97%	96.04%	99.44%	96.65%

$$(Xylan)_n + nH_2O \rightarrow nXylose \quad (2)$$

As a result of the data fit, the next equation was obtained:

$$X_{recov} = AT_p + Bt_p + CS_{\%} + DT_P^2 + Et_p^2 + FS_{\%}^2 + GT_p t_p + HT_p S_{\%} + It_p S_{\%} + JT_p t_p S_{\%} + KS_{\%}^2 T_p + LT_p^3 \quad (3)$$

where:

T_p = temperature inside reactor (°C);

t_p = pretreatment residence time (min);

$S_{\%}$ = sulfuric acid percentage;

X_{recov} = recovered fraction of glucan or xylan in pretreated solid.

The coefficients for Eqn (3) and their validity ranges are listed in Tables 2 and 3, respectively.

Enzymatic hydrolysis modeling The next reaction using this equipment was conducted at 50 °C:[48]

$$C_6H_{10}O_5 + H_2O \rightarrow C_6H_{12}O_6 \quad (4)$$

The next equation was obtained through a numerical regression process of data:

$$X_{G,H} = Ac_E + Bt_h + Cc_E^2 + Dt_h^2 + Ec_E t_h + Fc_E^3 + Gt_h^3 + Hc_E^2 t_h + Ic_E t_h^2 \quad (5)$$

Table 3. Validity interval of pretreatment models.

Pretreatment	Biomass	Variable	Interval	Source
Steam explosion	Sugarcane bagasse	T_p	160–190	[44]
		t_p	4–60	
	Corn stover	T_p	150–180	[45]
		t_p	5–25	
Dilute acid	Sugarcane bagasse	T_p	170–190	[46]
		t_p	5–15	
		$S_{\%}$	0.45–0.85	
	Corn Stover	T_p	190–210	[47]
		t_p	5–10	
		$S_{\%}$	0.01–0.5	

where:

c_E = cellulase-enzyme concentration (FPU g^{-1} glucan);

t_h = hydrolysis residence time (h);

$X_{G,H}$ = conversion fraction from glucan to glucose during enzymatic hydrolysis.The coefficients for Eqn (5) and their validity range are listed in Tables 4 and 5, respectively.

Fermentation modeling In this equipment, the next reaction was carried out at 32 °C employing the yeast *Saccharomyces cerevisiae* due to its tolerance to high ethanol concentrations and inhibitors:[36,51]

$$C_6H_{12}O_6 \rightarrow 2C_2H_6O + 2CO_2 \quad (6)$$

Table 4. Polynomial regression coefficients for enzymatic hydrolysis modeling.

	Steam explosion		Dilute sulfuric acid	
	Sugarcane bagasse	Corn stover	Sugarcane bagasse	Corn stover
		1.250 E+00		
A	1.506 E+00	2.788 E–01	4.470 E–01	1.377 E+01
B	1.226 E+00	1.650 E+00	1.987 E+00	2.609 E+00
C	5.300 E–03		8.780 E–02	–1.065 E+00
D	–1.379 E–02	–3.907 E–02	–2.839 E–02	–3.825 E–02
E	9.900 E–03	5.084 E–02	–1.250 E–02	–6.450 E–02
F				3.080 E–02
G	7.700 E–05	2.900 E–04	1.530 E–04	1.840 E–04
H				8.000 E–04
I	–1.960 E–04	–3.200 E–04		3.180 E–04
Coefficient of determination (R^2)				
	99.50%	98.57%	98.89%	99.82%

Table 5. Validity interval of enzymatic hydrolysis models.

Pretreatment	Biomass	Variable	Interval	Source
Steam explosion	Sugarcane bagasse	c_E	8–15	[49]
		t_h	4–96	
	Corn Stover	c_E	10–30	[50]
		t_h	2–72	
Dilute acid	Sugarcane bagasse	c_E	8–15	[49]
		t_h	4–96	
	Corn Stover	c_E	5–15	[48]
		t_h	2–96	

As a result of the data fit, the next equation was obtained:

$$X_{G,F} = Ac_G + Bt_F + Cc_G^2 + Dt_F^2 + Ec_G t_F + Fc_G^3 + Gt_F^3 + Hc_G t_F^2 \quad (7)$$

where:

c_G = glucose concentration at reactor inlet ($g L^{-1}$);

t_F = fermentation residence time (h);

$X_{G,F}$ = conversion fraction from glucose to ethanol during fermentation.The coefficients for Eqn (7) and their validity range are listed in Tables 6 and 7, respectively.

Ethanol purification modeling Ethanol separation modeling was carried out by selecting an extractive distillation sequence with glycerol as entrainer, and taking into account equipment costs and energy requirements.[53] The desired purity was 99.5% wt or more as this is the required purity for ethanol to improve physicochemical properties

Table 6. Polynomial regression coefficients for fermentation modeling.

A	9.68 E–01
B	–4.43
C	–1.15 E–03
D	4.066 E–01
E	6.61 E–02
F	1.6 E–05
G	9.07 E–03
H	1.032 E–03
Coefficient of determination (R^2)	
	98.82%

Table 7. Validity interval of fermentation model.

Variable	Interval	Source
c_G	50–100	[52]
t_F	1–24	

of biojet fuel.[10,12] This process was modeled and simulated in Aspen Plus 8.8, and nonrandom two-liquid (NRTL) model was selected as a thermodynamic model due to the presence of non-idealities in the ethanol/water mixture.[54] The rigorous simulation module of distillation columns in Aspen (RADFRAC) module with a Kettle-type reboiler and total condenser was used, and the total number of stages, the feed stages, the distillate/feed ratio, the reflux ratio, and the diameter of the columns were varied.

To meet sustainability goals, ethanol production was intensified. The intensification of ethanol separation

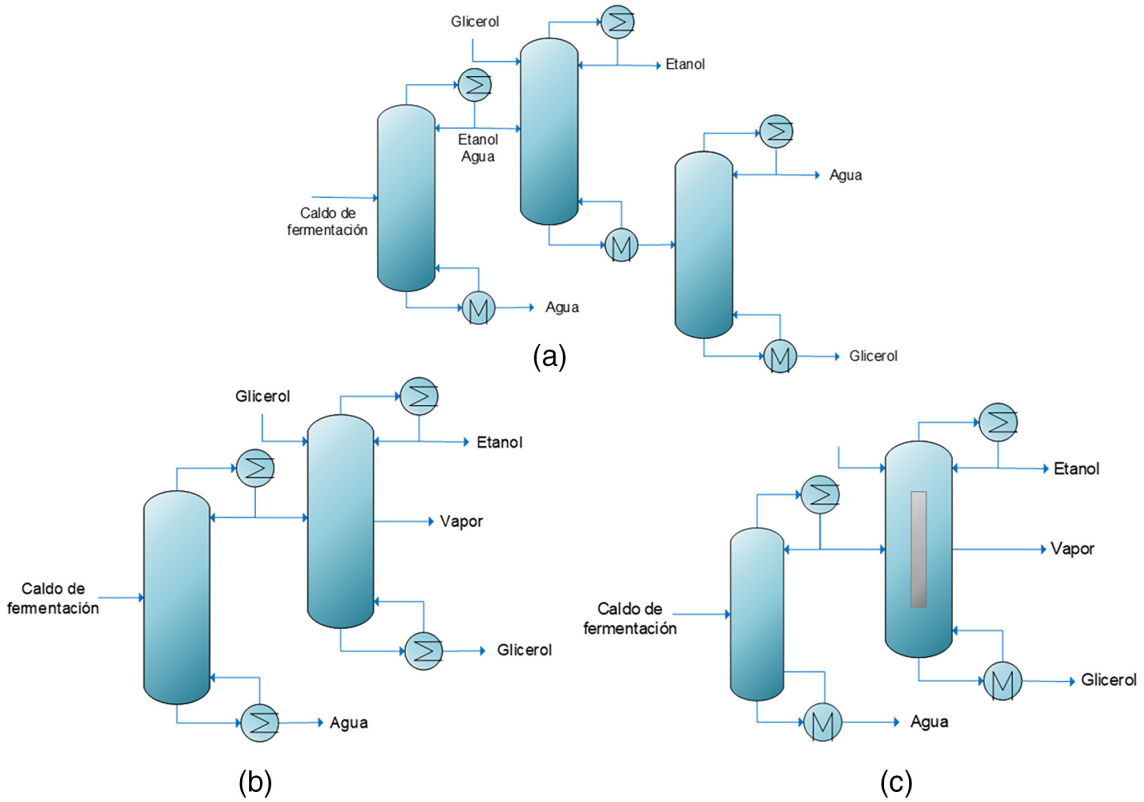

Figure 4. Ethanol separation alternatives: Conventional column sequence (a) column with vapor side stream (b), and dividing wall column (DWC) (c).

has been widely studied, and improvements in energy efficiency, cost savings, and environmental impact have been demonstrated successfully.[23-25,54,55] In this respect, a conventional column sequence (Fig. 4(a)) and a column sequence with vapor side stream (Fig. 4(b)) and a sequence with a dividing wall column (DWC) were proposed as separation schemes. This last configuration can be modeled as a thermally coupled column configuration (or Petlyuk column) (Fig. 4(c)), which is thermodynamically equivalent when there is no transfer energy through the dividing wall.[23,56] Aspen Plus 8.8 does not have a specific block for the DWC column, so this was modeled as a Petlyuk column which is the thermodynamic equivalent scheme for DWC. The dividing wall column (DWC) model was carried out in aspen plus using the rigorous distillation column (RADFRAC) module. For this particular case, two RADFRAC modules were required for the simulation to represent the DWC (Yildrim *et al.*[57]). The NRTL model was used with the RADFRAC module, varying the total number of stages, the feed stages, the distillate/feed ratio, the reflux ratio, and the diameter of the columns.

Biojet fuel process design

For the ATJ process, the design and data proposed by Byogy Renewables in 2011[58] were employed. The simulation was carried out in a similar way in Aspen Plus 8.8, making use of the unsymmetric electrolyte NRTL property method (ENRTL-RK) model due to the presence of electrolytic species in some zones of the process. The operational conditions of the reactors, as well as the block employed in Aspen Plus and their specifications, are given in Table 8. For those reactions whose conversion is specified, the reference component is written in bold.

For further information about yields in the oligomerization and hydrogenation stages, see Tables S1 and S2 in the Appendix S1, respectively.

At the final step, the jet fuel distillation was modeled in a RADFRAC block with a Kettle-type reboiler and total condenser, varying the total number of stages, the feed stages, the distillate flowrate, the reflux ratio, and the diameter of the column.

As can be seen, the anterior superstructure and the ATJ process are modeled with highly non-linear and potentially non-convex equations. The existence of degrees of freedom

Table 8. Operational conditions for reactors in ethanol-biojet process[58]

Stage	Block in Aspen	Reaction	*P* (bar)	*T* (°C)	Specification
Dehydration	RStoic	$C_2H_5OH \rightarrow C_2H_4 + H_2O$	8–14	320–500	Conversion 0.988
Oligomerization	RYield	—	40–55	350–470	Yield
Hydrogenation	RYield	—	8–15	145–240	Yield
Reforming					
Dry	REquil	$CH_4 + H_2O \rightarrow CO + 3H_2$ $CH_4 + CO_2 \rightarrow 2CO + 2H_2$	17–25	640–900	Temperature approach 400 °C
Steam (HTS)	RStoic	$CO + H_2O \rightarrow CO_2 + H_2$	15–20	340–520	Conversion 0.9
Steam (LTS)	RStoic	$CO + H_2O \rightarrow CO_2 + H_2$	11–20	175–250	Conversion 0.9

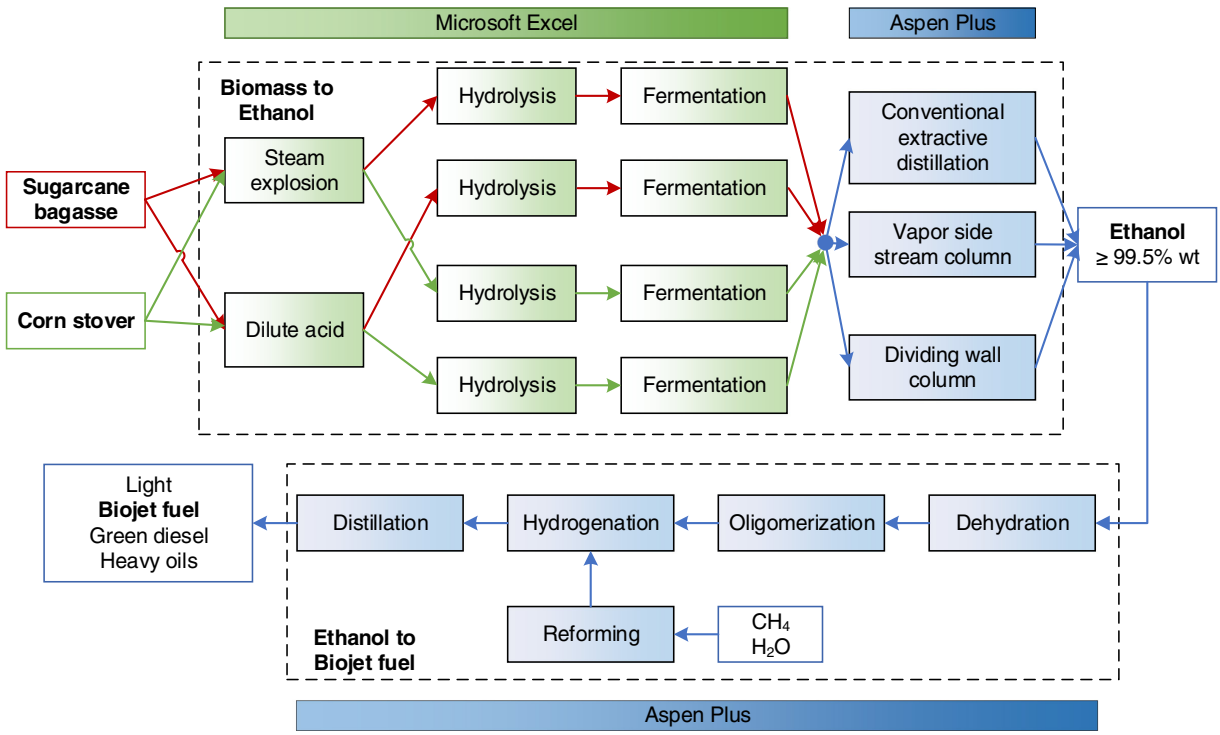

Figure 5. Complete superstructure for biojet fuel production process.

allows the design problem to be solved as an optimization problem. Finally, the superstructure to be optimized is shown in Fig. 5. As mentioned before, the reaction zone in the biomass-ethanol process was modeled in Microsoft Excel and the purification zone, as well as the entire ethanol-biojet process, was modeled in Aspen Plus. It is important to mention that this block diagram is not unique but it is going to be subjected to all possible combinations within the solution superstructure.

Process optimization

In accordance with the circular economy model, the search for appropriate technologies to convert lignocellulosic biomass into biojet fuel, as well as the design and operation parameters that maximize savings and minimize environmental impact, turn the design problem into a multi-optimization problem. When these two objectives are met, a sustainable process can be obtained. This is a profitable and greener process.

Objective functions

To assess the sustainability of the process in economic and environmental terms, the total annual cost (TAC) and Eco-indicator-99 (EI99) were selected as objective functions for both processes. Their benefits have been highlighted by several studies because they are

Table 9. Decision variables on biomass–ethanol process.

Variable	Planning	SB-SE	SB-DA	CS-SE	CS-DA	Purification		
						A	*B*	*C*
Cellulose amount	12 c							
X	12 c							
Y	12 c							
Z	12 c							
Temperature		8 c	8 c	8 c	8 c	1 c	1 c	1 c
Pressure		1 c	1 c	1 c	1 c			
Residence time		3 c	3 c	3 c	3 c			
Acid concentration			1 c		1 c			
Enzyme conc.		1 c	1 c	1 c	1 c			
Number of stages						3 d	2 d	3 d
Feed stage						3 d	2 d	2 d
Solvent stage						1 d	1 d	1 d
Reflux ratio						3 c	2 c	2 c
Distillate/feed ratio						3 c	2 c	2 c
Diameter						3 c	2 c	3 c
Solvent/feed ratio						1 c	1 c	1 c
Side stream stage								3 d
Interconnection flowrate								2 c
Total	48 c	13 c	14 c	13 c	14 c	11 c 7 d	8 c 5 d	11 c 9 d

Table 10. Decision variables on ethanol-biojet process.

Variable	Reforming	Dehydration	Oligomerization	Hydrogenation	Distillation
Pressure	6 c	2 c	1 c	1 c	1 c
Temperature	6 c	2 c	1 c	1 c	
No. of stages					2 d
Feed stage					1 d
Reflux					1 c
Distillate					1 c
Side stream flowrates					2 d
Diameter					2 c
Total	12 c	4 c	2 c	2 c	5 c 5 d

adequate indicators of the sustainability of a process and are in accordance with the criteria of the circular economy.[55,59-62] As previously mentioned, the proposal is to cover an annual demand of 5.5% of the biojet consumed in Mexico. In this sense, it is necessary to produce a sufficient amount of alcohol as raw material, to be transformed into biojet and cover the proposed demand.[31] This is expressed in Eqn (8):

$$F_{obj}\left(\vec{X}\right)=\{\begin{matrix}\min\left(TAC,EI99\right)\\ \max\left(\mathrm{EtOH}\right)\end{matrix}\quad s.t.\quad \vec{y}_k=\vec{x}_k \tag{8}$$

Tables 9 and 10 show detailed information about the decision variables involved in each operation for both

biomass-ethanol process and ethanol-jet process. The letter 'd' indicates that the variable is discrete and the letter 'c' indicates that the variable is continuous. The meaning of *X*, *Y*, and *Z* are the same as in Fig. 3. In the purification column, *A*, *B*, and *C* refer to conventional extractive distillation, vapor side stream scheme and the dividing wall scheme, respectively. In total, 132 continuous and 21 discrete variables were counted for biomass-ethanol process. For the ethanol-biojet process, 25 continuous and five discrete variables were also counted.

Total annual cost

The TAC allows the quantification of the economic performance of a process when it is under development. It stands out as an indicator of the economy of the process because it is based not only on the product but on the characteristics of the process for informational and comparative purposes.[59] The total cost objective function includes the operating costs for heating and cooling utilities, as well as the capital costs of the equipment.[63] In addition, Quiroz-Ramírez *et al.*[62] include, within the operating costs, the cost of electricity and supplies.

The objective function of total annual cost is calculated according to Eqn (9):

$$TAC(\$USD/kg) = \frac{\frac{\sum_{i=1}^{n} C_{TM\,i}}{t_{ri}} + \sum_{j=1}^{m} C_{ut_j}}{F_k} \tag{9}$$

where C_{TM} represents the total cost of the *i*-module, C_{ut} is the cost of *j*-utility, t_{ri} is the payback period (3 years), and F_k is the reference flow.

Prices of supplies are provided in Appendix A1.

Ecoindicator-99

The Eco-indicator-99 is a quantitative index proposed as part of the methodology of the same name for life cycle analysis.[64] This methodology contemplates the life of a product from the origins of the raw material, during its process, and in its degradation. It is based on the use of standard ecological indicators, which are numbers that express the total environmental load of a product or process. The larger the indicator, the greater the environmental impact.[59] This methodology is divided into three impact categories: human health, ecosystem quality, and resource depletion. It is calculated with Eqn 10:

$$EI99(ecopts/kg) = \frac{\sum_b \sum_d \sum_{k\in K} \delta_d \omega_d \beta_b \alpha_{b,k}}{F_k} \tag{10}$$

where β_b is the total amount of chemical *b* released per unit of reference flow due to direct emissions, $a_{b,k}$ is the damage caused in category *k* per unit of chemical *b* released to the environment, ω_d is a weighting factor for damage in categories *d*, and d_d is the normalization factor for damage of category *d*. The unit of measurement employed for EI99 is the ecopoint, where 1 ecopoint represents one-thousandth of the annual environmental load of an average European inhabitant.[55,59]

Values of unit Eco-indicators in their impact categories are provided in Appendix A2.

Stochastic optimization

In terms of mathematical optimization methods, deterministic and stochastic methods can be used to solve high-dimensional, non-linear problems within a complex search space. On the one hand, deterministic methods require the calculation of first and/or second derivatives of the objective function and its constraints equations. These methods are strongly dependent on the initial solution chosen in the search for the optimal solution. On the other hand, stochastic methods have the advantage of not requiring the manipulation of the mathematical structure of the objective function and its constraints, allowing the equations to be employed in their explicit form and not requiring an initial feasible point. One of the stochastic methods that have shown to be able to solve highly non-linear and potentially non-convex problems is differential evolution with a tabu list (DETL).[65]

Differential evolution with a tabu list

The stochastic optimization method of differential evolution with a tabu list (DETL)[66] stands out among other stochastic methods for its robustness, that is, its ability to locate the global optimum regardless of the parameters of the problem, its small number of evaluations of the target function, and its efficiency in terms of computation times. The DETL method showed that the use of some concepts of the metaheuristic tabu can improve the performance of the differential evolution algorithm. In particular, the tabu list is used to avoid the revisit of search space by keeping a record of recently visited points, which can avoid unnecessary function evaluations. This is what provides to the method its high time efficiency.[65–68] The proper functionality of this technique has been proven when applied to intensified systems of separation and reactive distillation.[60,65,69–72]

The algorithm is shown in Fig. 6 and works as follows: each individual is represented as a vector of decision

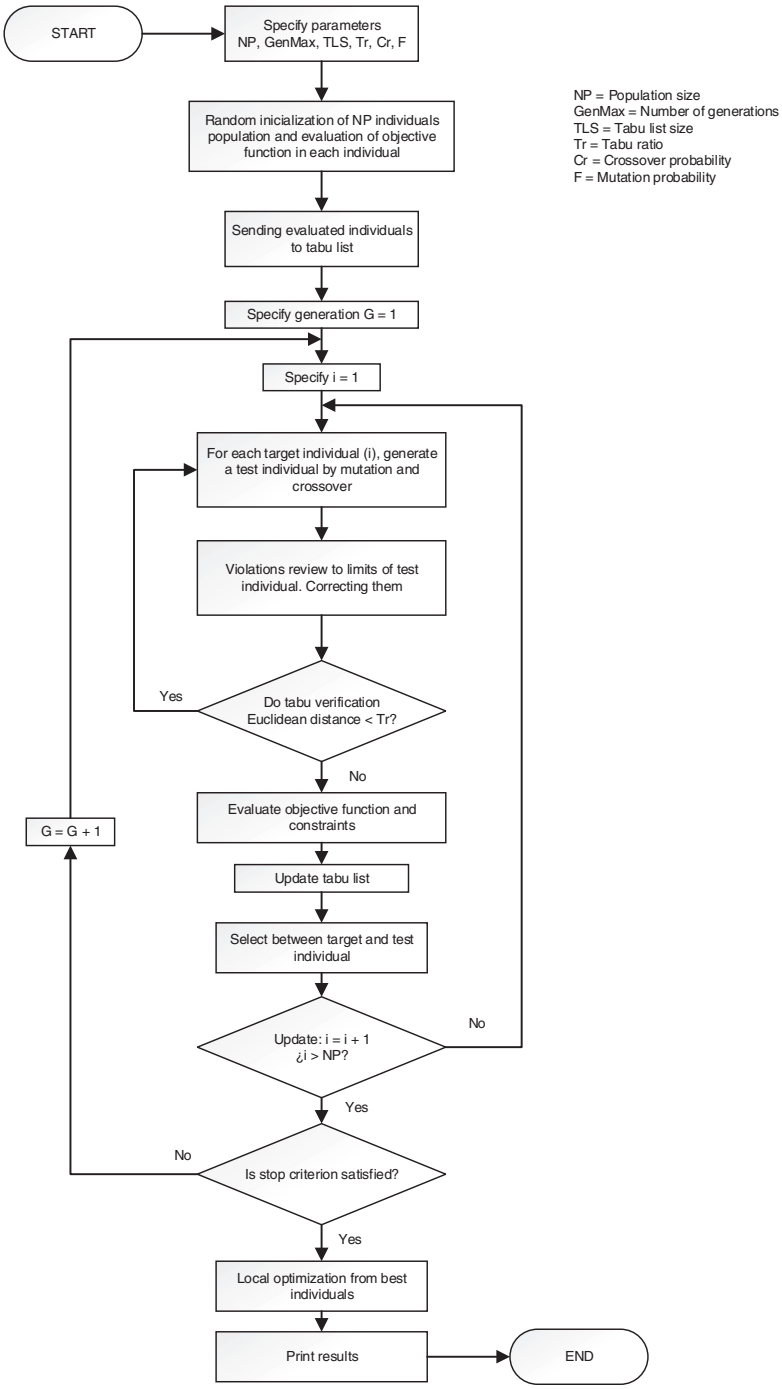

Figure 6. Multiobjective optimization algorithm by differential evolution with tabu list.

variables becoming part of an initial random population of population size (NP) individuals generated within the limits of the decision variables. Then, the value of target functions and constraints is calculated for each individual in the initial population. The tabu list is filled with 50% of the individuals in the initial population, and the initial individuals are identified as target individuals (*i*). Subsequently, one test individual is generated for each target individual by mutation and crossover of three random individuals from the initial/current/parental population. Elements of the mutant vector compete with those of the target vector with a *Cr* probability of generating a test vector. At this point a tabu check is implemented: if the test individual is close to any

individual in the tabu list for a specified distance Tr (tabu ratio), it is rejected without calculating the objective functions and constraints. This will happen until the test individual is far away from any individual on the tabu list. Next, the Euclidean distance between the test individual and each individual in the tabu list in the decision variable space to accept the test individual is calculated. Then, objective functions and constraints are calculated for the temporarily accepted test individual. After generating test individuals for all target individuals in the current population, if necessary, an undivided classification of current and combined offspring populations is performed followed by the calculation of the agglomeration distance to select the next generation individuals. Thus, the best NP individuals are used as the population in the subsequent generation.[73]

Implementation of the optimization algorithm

The stochastic optimization method was implemented using a hybrid platform that incorporated Microsoft Excel and Aspen Plus 8.8. In it, a vector of decision variables is sent to Microsoft Excel by using a dynamic data exchange with Component Object Model (COM) technology. In Microsoft Excel, such values are attributed to process variables required by Aspen Plus 8.8. Once the simulation is completed, Aspen Plus returns the resulting vector to Microsoft Excel. Finally, Microsoft Excel analyzes the values of the objective function and proposes new values of the decision variables according to the stochastic optimization method.[55] This type of tool, illustrated in Fig. 7, has been applied successfully to process design and optimization.[55,61,62,74] The surrogate models in Excel are called through a subroutine inside Visual Basic within Microsoft excel. In the same way, the link between Excel and Aspen Plus is developed using Visual Basic as a carrier information platform. For more detail about this link, a deeper explanation is provided in Segovia-Hernandez and Gomez-Castro.[75]

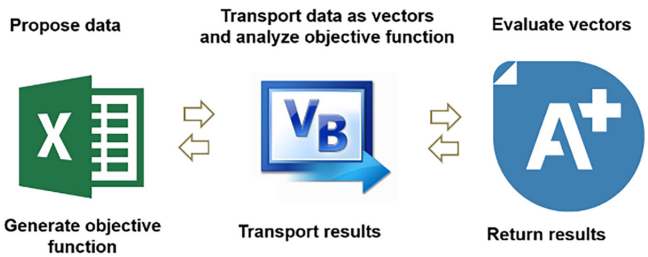

Figure 7. Hybrid platform for DETL stochastic optimization.

According to Ng and Maravelias[28] the efficiency of the biofuel biorefinery, in terms of both cost and CO_2 emissions, can be improved by the installation of depots (sections) and the optimization of each depot for the transformation of biomass to biofuel. Based on the ideas of Bowling *et al.*[26] and Ng and Maravelias,[27,28] which establish that the distributed configuration has a lower cost than the centralized configuration for the design of a biorefinery, we decided to divide the optimization of the biorefinery under study into two sections: the conversion of biomass to bioethanol and the transformation of bioethanol to bio jet fuel. The parameters required by the method are reported in Table 11.

Results and discussion

As stated in the section on 'Process modeling', the entire process is analyzed in two parts: the biomass-ethanol process and the ethanol-biojet process.

Feedstock planning

Figure 8 shows the annual amount of sugarcane bagasse and corn stover that are pretreated by steam explosion and dilute acid and required to produce the optimal flow of ethanol. It is important to consider that both types of pretreatments were considered to be appropriate pretreatments for the transformation of the biomass considered here, with the intention that the optimization method would select the best alternative to meet the objectives considered in the optimization problem. This consideration is consistent with other types of biorefinery designs as reported by El-Halwagi *et al.*[76] and Santibañez-Aguilar *et al.*[77] In total, 8 357 524 ton $year^{-1}$ of sugarcane bagasse are required, of which 46% is sent to steam explosion and 54% to acid pretreatment; and 408 970 ton $year^{-1}$ of corn stover, of which 28% is subjected to steam explosion and 72% to acid pretreatment.

It is observed that, in the optimal solution, it is required to use a greater amount of sugarcane bagasse compared to the amount of corn stover. This is explained by the

Table 11. Parameters of the optimization method.

Population size	Number of generations	Tabu list size	Crossover probability	Mutation probability	Tabu ratio
120	1000	60	0.9	0.3	0.0001

fact that it is more expensive to process corn stover in reaction trains involving both pretreatments. Thus, the optimization method compensates this effect by raising the requirements for sugarcane bagasse. The same observation applies to Eco-indicator-99. The processing of corn stover by both routes results in a greater environmental impact than sugarcane bagasse. Again, to minimize this effect the method is oriented to choose the sugarcane bagasse as the most appropriate feedstock. In addition, sugarcane bagasse has a higher content of hexoses sugars and its cost is lower than that of corn stubble, so the optimization method tends to choose it as the best feedstock.

Figure 9 shows the distribution of the raw material during the year. It can be observed that there is a tendency for the optimization method to choose sugarcane bagasse processed with diluted acid. This is attributed to the bagasse/acid combination offering better performance with a low TAC and EI99 as shown in Table 12.

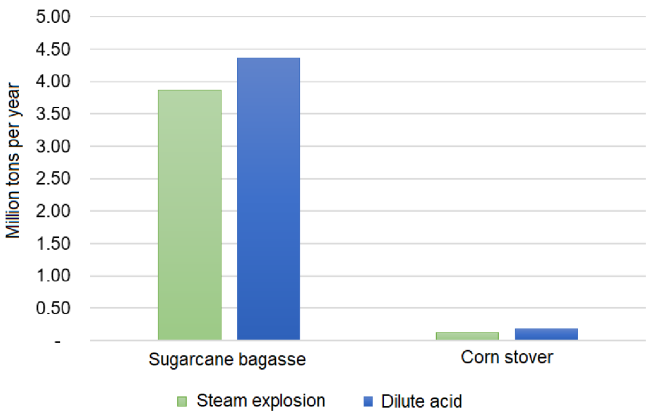

Figure 8. Annual biomass requirement in steam explosion and dilute acid processes. Green colour - Steam explosion, Blue - Dilute acid.

Optimization of ethanol process

Figure 10 shows the Pareto front for optimal ethanol production. At the optimum, the maximum production of ethanol was achieved at 79 894 kg h^{-1} (679 100 ton $year^{-1}$) with a purity greater than 99.5% by weight. There is a clear compromise between the objective economic and environmental impact functions for the conventional and intensified separation sequences. It can be observed that, for the conventional sequence, (*A*) a minimum TAC and EI99 of 1.295 USD kg^{-1} ethanol and 0.4716 ecopoints kg^{-1} ethanol were achieved, respectively. On the other hand, the column sequence with a vapor side stream (*B*) obtained an optimal level of 1.223 USD kg^{-1} ethanol and 0.4635 ecopoints kg^{-1} ethanol. This represents a reduction of 5.56% in the TAC and 1.72% in the Eco-indicator in comparison with the conventional sequence. Finally, with the dividing wall column sequence (*C*) a TAC of 1230 USD kg^{-1} ethanol and an EI99 of 0.4578 ecopoints kg^{-1} ethanol were obtained. In the same sense, the dividing wall scheme achieved a saving of 5.02% in the TAC and a decrease of 2.92% in the value of the ecoindicator in relation to the values obtained in the conventional sequence.

An interesting observation relates to the Pareto front of sequence *C*. Between the *C*2 and *C*3 designs, the difference between the Eco-indicators is in the order of 10^{-4}, whereas the difference between the TACs is 0.014. That is, the difference from the EI99 is not significant enough to rule out the *C*3 design as better than the *B*2 design. However, from a utopian point of view, the optimal design of sequence *C* is around point *C*2.

Table 13 shows a summary of the optimal objective functions for the biomass – ethanol process (with separation sequence) for the conventional separation case (Sequence *A*), column sequence with vapor side stream (Sequence *B*), and the dividing wall column sequence (Sequence *C*).

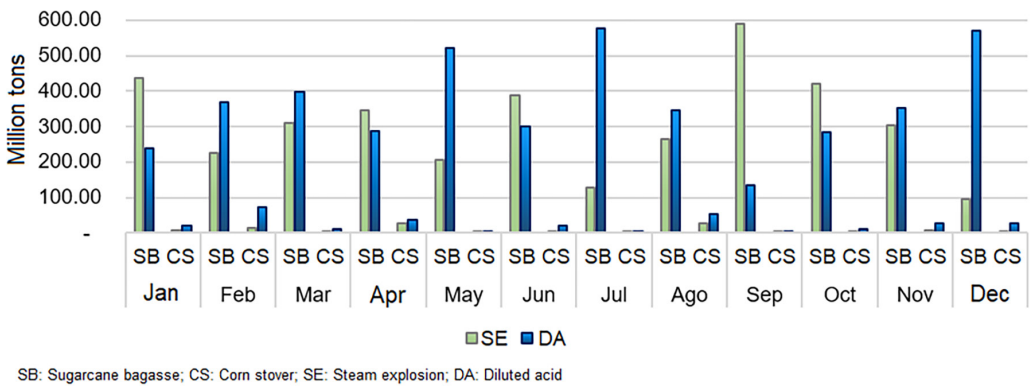

Figure 9. Annual feedstock planning. Green - Steam explosion, Blue - Diluted acid. CS, corn Stover; DA, diluted acid; SB, sugarcane bagasse; SE, steam explosion.

Table 12. Yield (kg ethanol kg^{-1} dry biomass).

	Sugarcane bagasse	Corn stover
Steam explosion	14.70	14.80
Diluted acid	16.13	17.05

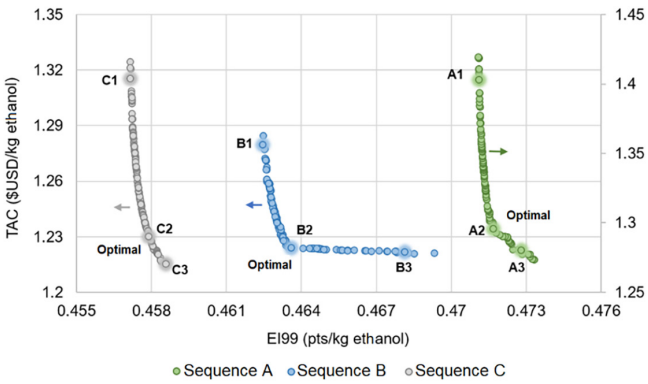

Figure 10. Pareto front for the biomass–ethanol process (with separation sequence) for the conventional separation case (sequence a), column sequence with vapor side stream (sequence *B*), and the dividing wall column sequence (sequence *C*). The highlighted points 1 to 3 correspond to the extremes of the Pareto; the most expensive with the lowest environmental impact (1), the cheapest with the highest environmental impact (3), and the most balanced (2). Green - Sequence A, Blue - Sequence B, Gray - Sequence C.

It may be observed that the most economical configuration is the column sequence with vapor side stream (*B*). However, from the environmental point of view, the sequence with dividing wall column (*C*) is the best alternative. Figure 11 shows how the amount of solvent is the most influential factor in the operational costs of distillation sequences. It contributes about 75% to the total cost of each separation sequence. It is also noted that sequence *B* uses less solvent than sequence *C*, which is why it is the most economical option. This can be attributed to the reduction in the reboiler duty in the dividing wall column which, to achieve the desired purity, is compensated with a greater amount of solvent, as will be discussed below.

Continuing with Fig. 10, in all three cases the total annual cost decreases as the eco-indicator increases. To find the reason for this behavior, three designs are considered in each sequence and analyzed according to their design parameters. These are shown in Figs 12, 13, and 14 for sequences *A*, *B*, and *C*, respectively. It is observed that, for the three schemes, the duty is increased with the reflux ratio, which is a behavior

Table 13. Optimal objective functions.

	A	*B*	*C*
TAC (USD kg^{-1} ethanol)	1.295	1.223	1.230
Percentage reduction		5.56	5.02
EI99 (pts kg^{-1} ethanol)	0.4716	0.4635	0.4578
Percentage reduction		1.72	2.92

common to distillation processes. Comparing the data reported in these tables with the Fig. 15, it is observed that designs with a higher Eco-indicator tend to operate with higher reflux ratios, higher duties, and, therefore, greater amounts of steam, which contributes to an increase in the EI99. This is because steam generation involves the burning of fossil fuels, which directly influences the eco-indicator as shown in Fig. 15.

As mentioned above, the amount of solvent, shown as the solvent/feed ratio, decreases as the reboiler duty of the second column increases, possibly as compensation to achieve the desired ethanol purity. This effect is observed in sequences *A*, *B*, and *C*. In the case of sequence *B*, the solvent ratio stabilizes at the lowest cost, as seen in Fig. 16.

Finally, sequence *B*2 was selected as optimal and the rest of the process was designed based on the results obtained by this configuration.

Optimization of the biojet fuel process

Figure 17 shows the Pareto front for optimization of the biojet fuel production process from ethanol. In the Pareto front, the extremes are highlighted, considering the upper left point (*D*1) as the point with a higher economic impact, but lower environmental impact; the lower right point (*D*3) is the point with a lower economic impact but a higher environmental impact; and finally, there is the point with the best balance between the evaluated objectives (*D*2). This selection of endpoints and the most balanced one will be very useful in later analyses. In this case, a minimum TAC of 0.275 USD kg^{-1} biojet fuel and a minimum EI99 of 70.18 ecopoints kg^{-1} biojet fuel were achieved for the most balanced alternative. This Eco-indicator value is attributed to the greater environmental impact inherent in the presence of hydrocarbons in the process. Finally, this design is capable of producing 224,206 ton per year (266,912 m^3 per year) of biojet fuel, which meets the 5.72% demand required for use in the case of fossil jet fuel in Mexico.

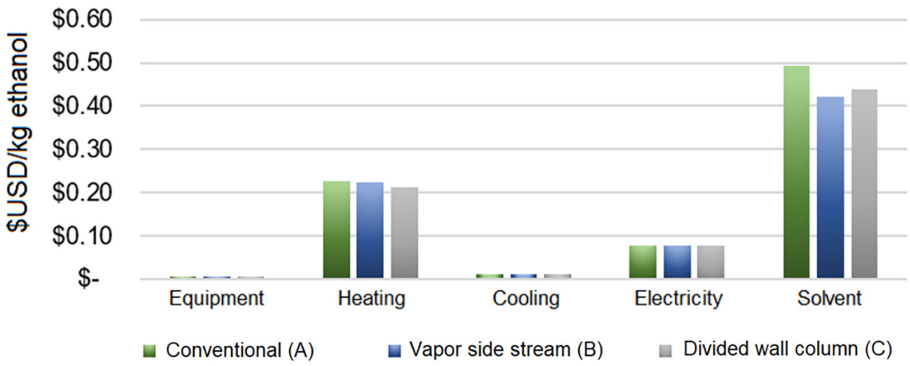

Figure 11. Total annual cost analysis for separation sequences at the optimal point. Green - Conventional (A), Blue - Vapor side stream (B), Gray - Divided wall column (C).

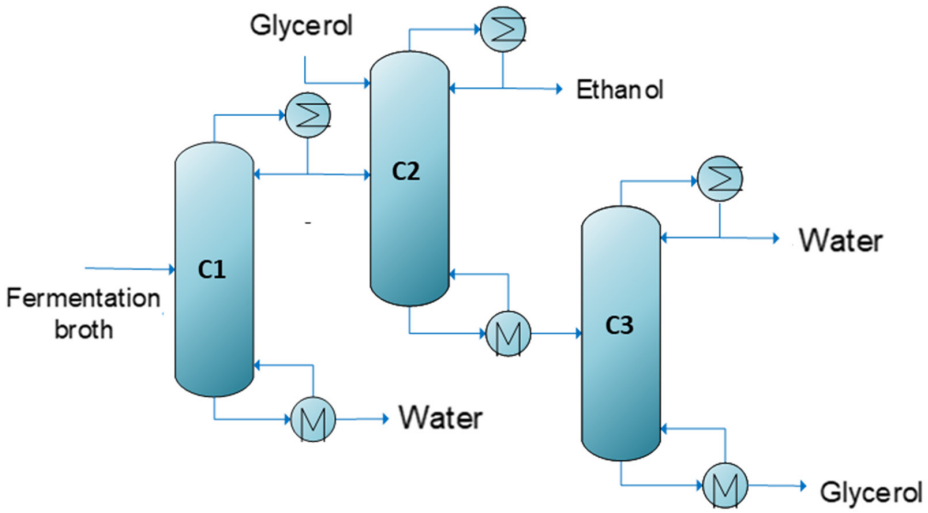

		A1	A2	A3
Column 1 (C1)	Reflux ratio	1.678	1.712	1.878
	Diameter	0.705	0.609	0.911
	Duty (MW)	160.27	160.65	163.97
Column 2 (C2)	Solvent/Feed ratio	0.72	0.589	0.564
	Reflux ratio	0.32	0.466	0.501
	Diameter	0.855	0.806	0.797
	Duty (MW)	28.97	30.86	31.42
Column 3 (C3)	Reflux ratio	0.106	0.122	0.125
	Diameter	0.848	0.999	0.988
	Duty (MW)	9.48	8.68	8.3
	Total duty (MW)	198.72	200.19	203.69
	TAC	1.403	1.296	1.278
	EI99	0.4711	0.4717	0.4728

Figure 12. Design parameters for the conventional scheme to purify ethanol (A), the lowest environmental impact (*A*1), the cheapest with the highest environmental impact (*A*3), and the most balanced (*A*2).

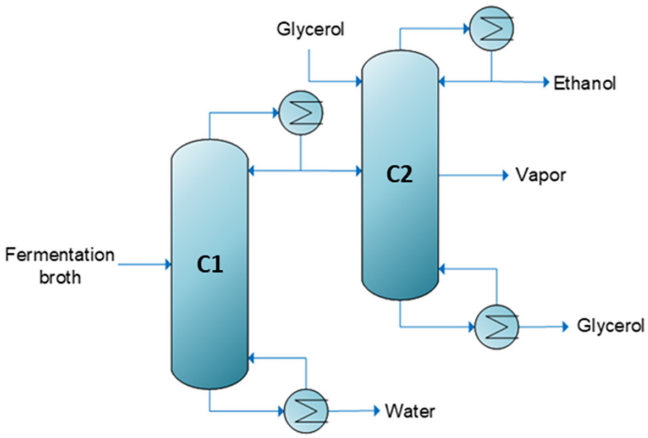

		B1	B2	B3
Column 1 (C1)	Reflux ratio	1.66	1.66	1.654
	Diameter	0.755	0.761	0.745
	Duty (MW)	160.661	160.684	158.577
Column 2 (C2)	Solvent/Feed ratio	0.573	0.504	0.504
	Reflux ratio	0.508	0.691	0.713
	Diameter	0.991	0.966	0.991
	Duty (MW)	40.198	43.155	43.18
	Total duty (MW)	200.86	203.84	201.76
	TAC	1.28	1.224	1.222
	EI99	0.4625	0.4636	0.4681

Figure 13. Design parameters for the scheme with a side stream column (*B*), the lowest environmental impact (*B*1), the cheapest with the highest environmental impact (*B*3), and the most balanced (*B*2).

The objective functions do not show a significant variation along the Pareto front, so that any point would represent equivalent designs, that is, it is a flexible design since, despite the change in operating conditions, economic and environmental indicators do not vary substantially. However, an analysis of the Eco-indicator reveals that the main source of environmental impact is the flow of processed hydrocarbons in the areas of dehydration, oligomerization, distillation, and hydrogenation, as shown in Fig. 18 for the optimal point. This is why, in contrast with the biomass-ethanol process, there are high Eco-indicator results.

In terms of total annual cost, the largest contribution is attributed to the costs of heating utilities, which account for about 75% of operating costs and 50% of the TAC. Taking the three points indicated on the Pareto front and breaking down their costs in Fig. 19, it is possible to observe that the decrease in the TAC can rather be

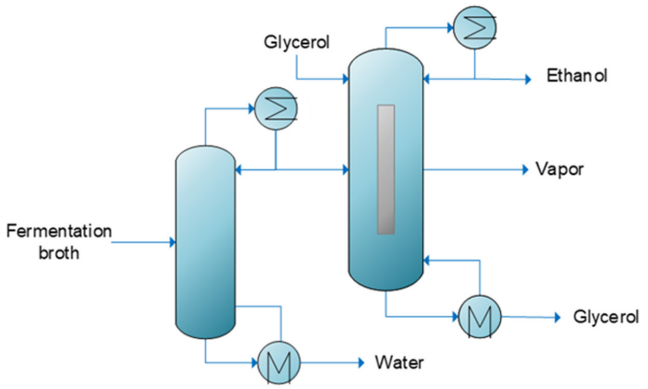

		C1	C2	C3
Column 1 (C1)	Reflux ratio	1.66	1.659	1.654
	Diameter	0.755	0.739	0.802
	Duty (MW)	160.661	160.674	158.286
Column 2 (C2)	Solvent/Feed ratio	0.626	0.522	0.503
	Reflux ratio	0.515	0.697	0.798
	Diameter	1.215	0.983	0.927
	Duty (MW)	18.722	20.73	22.41
	Total duty (MW)	179.383	181.403	180.695
	TAC	1.316	1.23	1.215
	EI99	0.4572	0.4579	0.4586

Figure 14. Design parameters for the scheme with a dividing wall column (*C*), the lowest environmental impact (*C*1), the cheapest with the highest environmental impact (*C*3), and the most balanced (*C*2).

attributed to a reduction in the cost of equipment and the heating utilities.

In the end, the complete process flow diagram is shown in Fig. 20. It can be observed that the vapor side stream column configuration is implemented. The optimal design and operating conditions that maximize ethanol production and minimize TAC and EI99 are specified.

Minimum selling price

The various factors that affect the economic and environmental performance of both process modules, biomass – ethanol and ethanol – biojet fuel have been analyzed. Lower annual costs occur with high Eco-indicators. Under these circumstances, the information provided by the Pareto fronts is not enough to know how profitable a design is if the minimum selling price of biofuel for such a design is not known.

In this section, an analysis of the sales price of biojet fuel is performed based on the different designs of the biomass–

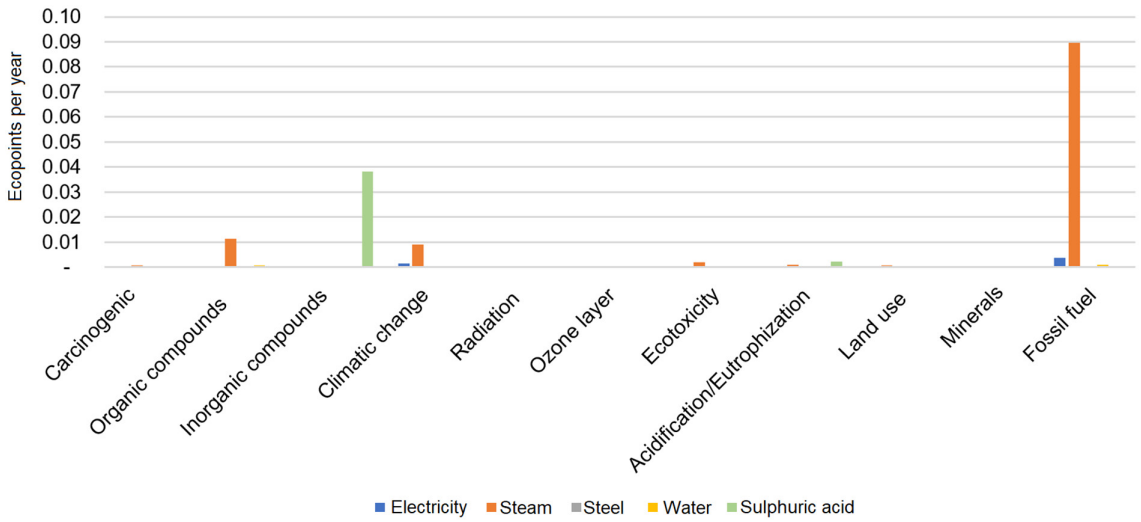

Figure 15. Ecoindicator-99 analysis for reaction – separation sequence *B* (separation alternative with a side stream column). Green- Sulphuric acid, Blue - Electricity, Gray - Steel, Yellow - Water, Red - Steam.

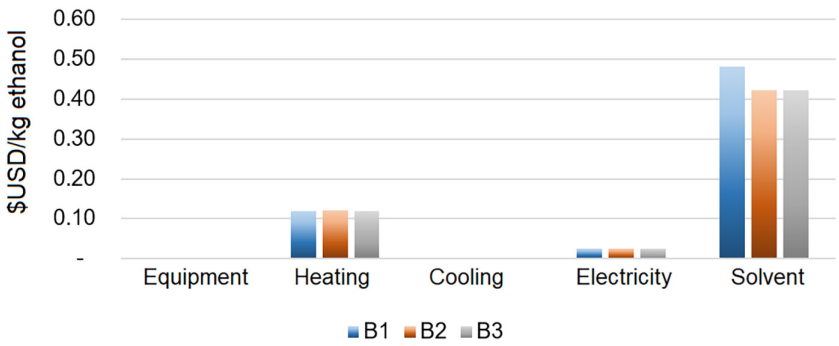

Figure 16. Analysis of the total annual cost for the process with vapor side stream (sequence *B*). The points 1 to 3 correspond to the extremes of the Pareto in Fig. 10; the most expensive with the lowest environmental impact (1) the cheapest with the highest environmental impact (3), and the most balanced (2). Blue - B1, Red - B2, Gray - B3.

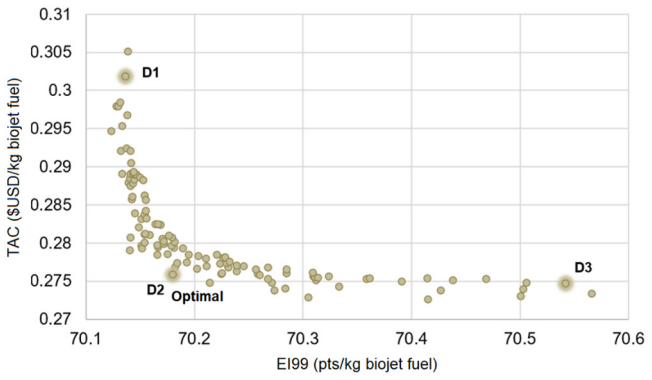

Figure 17. Pareto front for ethanol–biojet fuel process. The points *D*1 to *D*3 correspond to the extremes of the Pareto in Fig. 10; the most expensive with the lowest environmental impact (*D*1), the cheapest with the highest environmental impact (*D*3), and the most balanced (*D*2).

ethanol process and taking the three points indicated on the Pareto front for the production of biojet fuel, in Fig. 17.

Figure 21 shows the sales prices of biojet fuel for the various scenarios presented. Note that lower sales prices were achieved with both intensified processes, *B* and *C*. However, it is necessary to make some observations. On the one hand, between designs *B*2 and *C*2, the one with the lowest selling price is *B*2. This coincides with the Pareto fronts shown in Fig. 10, in which the design with vapor side stream column exhibits the lowest TAC. On the other hand, globally, design *C*3 exhibits the lowest selling prices. This is associated with the fact that this design has the lowest TAC of those presented in Fig. 10. However, as mentioned previously, from a utopian point of view, design *C*2 is optimal. Although design *C*3 has the lowest selling price, it is not yet profitable, which will be discussed later.

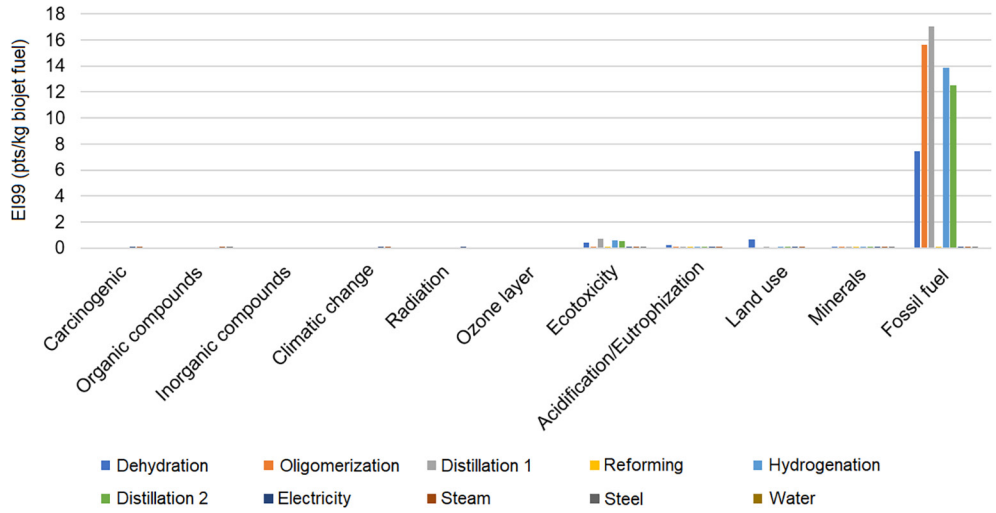

Figure 18. Ecoindicator-99 analysis for ethanol–biojet fuel process. Green - Distillation 2, Blue - Dehydration , Gray -Distillation 1, Yellow - Reforming, Red - Steam, Orange - Oligomerization, Brown - Water, Black - Steel, Navy Blue - Electricity.

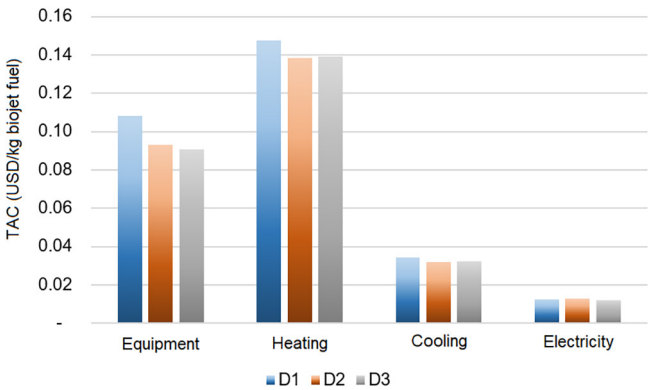

Figure 19. Total annual costs analysis for the ethanol–biojet fuel process, representing the extremes of the Pareto front in Fig. 14: The most expensive with the lowest environmental impact (*D*1), the cheapest with the highest environmental impact (*D*3), and the most balanced (*D*2). Green - D1, Blue - D2, Gray - D3.

Figure 21(b), which corresponds to the optimum point of the ethanol–biojet fuel process, shows that the lower sales prices between the optimal points *A*2, *B*2, and *C*2 were achieved with design *B*2. This behavior was expected as the lowest TAC was obtained with this design. At the optimum point *B*2-*D*2 the minimum selling price was USD 1.653 L^{-1}. The sale price of conventional jet fuel in Mexico in 2020 was USD 0.414 L^{-1} of jet fuel. This is an indicator that the entire process is not profitable because the minimum selling price of biojet fuel is four times higher than the selling price of fossil jet fuel. The amount of the solvent contributed greatly to this, as mentioned in the TAC analysis in the section headed 'Optimization of the ethanol process'. One way to reduce this cost is to integrate glycerol into extractive distillation as a by-product of a biodiesel biorefinery. This would avoid the purchase of the solvent and, within the framework of a biorefinery, it would be fed to the process as a by-product of a previous process. In this sense, the glycerol obtained from the production of biodiesel has a price between 0.09 and 0.20 USD kg^{-1}, while the glycerol obtained by other routes has a price between 0.60 and 0.91 USD kg^{-1}.[78]

The scenario observed when comparing the selling prices of biojet produced from fossil sources compared to that produced from renewable lignocellulosic material is not very encouraging. Generating an adequate and competitive selling price compared to a synthetic route presents several challenges. From a microbiological point of view, a major challenge at present lies in the development of strains with a high tolerance to ethanol. Alcohol is a product of strain metabolism, a toxic product. In that sense, the development of a strain that is highly resistant to alcohol concentration directly represents a fermentation broth with higher ethanol concentration. This higher concentration would generate less energy investment in ethanol purification, which would reduce the costs associated with ethanol purification significantly. A greater amount of ethanol would also be generated, with a greater amount of biojet, which would imply a lower cost per kilogram of biojet produced. This would result in a lower cost of sale of the biojet. Of course, the search for more efficient separation technologies with lower energy consumption continues to be a constant quest in the synthesis, modeling, and optimization of processes.

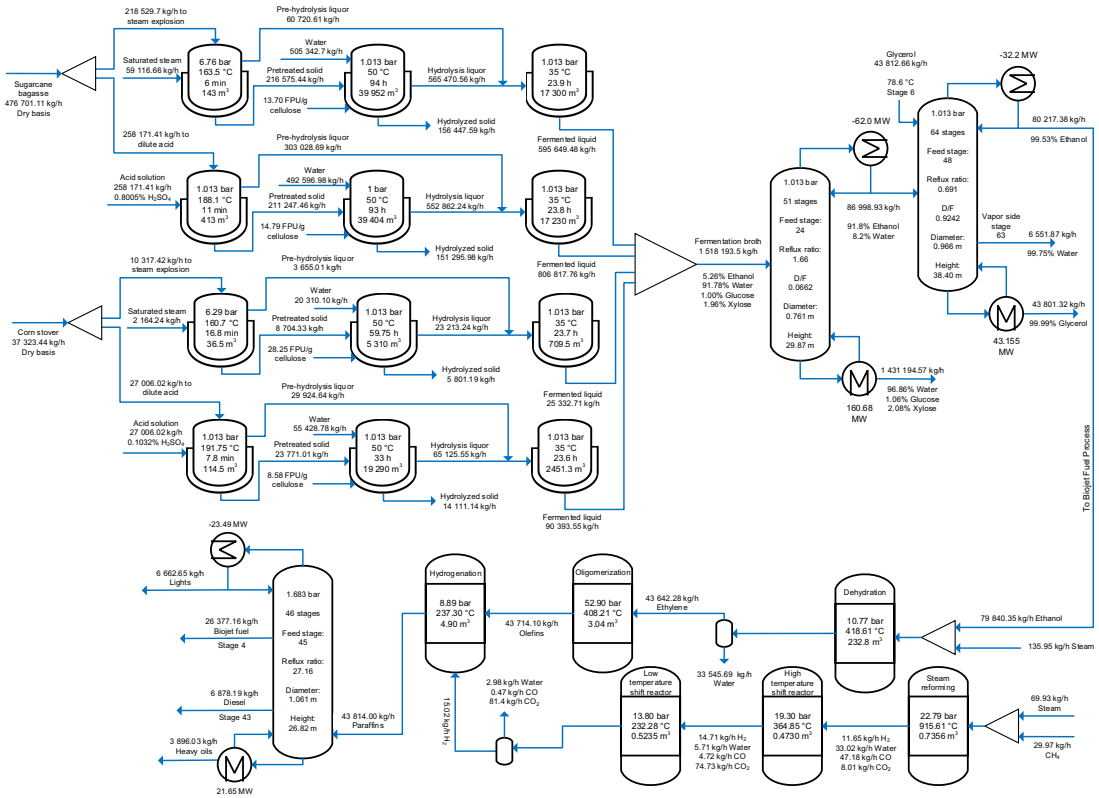

Figure 20. Process flow diagram with optimal configuration for biomass–ethanol–biojet fuel process.

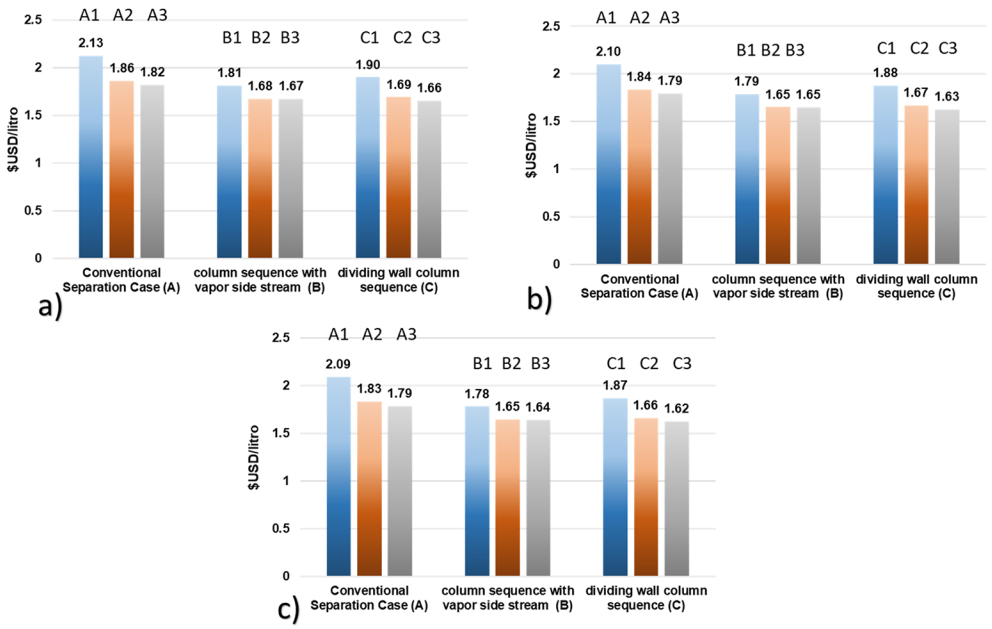

Figure 21. Minimum selling price of biojet fuel (straight line) compared to the extremes of the Pareto front presented as a solution of the ethanol–bio jet process in Fig. 10, the most expensive with the lowest environmental impact (a), the cheapest with the highest environmental impact (c) and the most balanced (b).

Conclusions

An intensified process of biojet fuel production was designed by the route of alcohols produced from lignocellulosic biomass under the concept of distributed configuration. By simulating the process, it was found that it can produce 266 912 m^3 $year^{-1}$ of biofuel, an amount that satisfies 5.72% of the national demand for conventional jet fuel in Mexico and is greater than the production needed by 2024 estimated by SENER[31] and Clúster Bioturbosina, CEMIE-Bio, (2015), Anexo IV Plan de Negocios, México. The previous result (shown in the results analysis) was achieved with solutions capable to meet sustainable criteria.

Regarding the raw material used to produce jet fuel, a very marked tendency of the optimization method to select sugar cane over corn stover was observed. This selection is totally influenced by several factors such as the cost of the raw material, the amount of fermentable sugars, the yield of each raw material, and its environmental impact. There was also a marked tendency to use dilute acid as a pretreatment method. Although it is not the one that offers the best yield, the cost associated with this pretreatment makes it the one with the best cost-performance ratio.

With the intensification of the ethanol purification process, it was observed that the most economically feasible configuration was that of a column with a vapor side stream. This achieved savings of 5.56% in the TAC and a 1.72% reduction in the EI99. In contrast, the configuration with dividing wall column achieved a greater reduction in the Eco-indicator, of 2.92%; and lower savings in the TAC, of 5.02%. It was identified that the cost of the solvent contributed to 75% of the total annual cost of each purification sequence. Analysis of the amount of solvent involved in each configuration revealed that the column scheme with vapor side stream used less solvent than the dividing wall column scheme.

The scheme with a dividing wall column did not present significant changes in the EI99 and design *C*3 presented a better economic and environmental performance than design *B*2. However, from a utopian point of view the optimal design is in the vicinity of point *C*2. Regarding the ethanol–biojet fuel process, the high values of the Eco-indicator were related to the inherent environmental impact caused by the presence of hydrocarbons in each of the operations of the process.

Regarding global bio jet production, a minimum TAC of 0.275 USD kg^{-1} biojet fuel and a minimum EI99 of 70.18 ecopoints kg^{-1} biojet fuel were achieved. This Eco-indicator value is attributed to the greater environmental impact inherent in the presence of hydrocarbons in the process. Finally, this design can produce 224 206 ton $year^{-1}$ (266 912 m^3 $year^{-1}$) of biojet fuel, which meets a 5.72% demand for conventional jet fuel in Mexico. With regard to the environmental impact, the Eco-indicator reveals that the main source of environmental impact is the flow of processed hydrocarbons in the areas of dehydration, oligomerization, distillation, and hydrogenation.

In terms of TAC, the largest contribution is attributed to the costs of heating utilities, which account for about 75% of operating costs and 50% of the TAC. At the optimum point for bio jet production, the minimum selling price was USD 1.653 $L.^{-1}$ The sale price of conventional jet fuel in Mexico in 2020 was USD 0.414 L^{-1} of jet fuel. This is an indication that the entire process is not profitable as the minimum selling price of biojet fuel is four times higher than the selling price of fossil jet fuel.

To make the process profitable, some actions are recommended. The integration of hydrolysis and fermentation into a single equipment is planned. In addition, the results obtained for intensified separation sequences show a considerable reduction in the Eco-indicator. This same effect is expected to be observed when implementing intensified systems in the ethanol–biojet fuel module, which, as observed, has a high environmental impact. Similarly, this innovation would reduce the capital costs of this section.

Regarding the profitability of the process, it is recommended to lower the sales price of biojet fuel not only by implementing intensification strategies in both processes but by exploring other feedstock options that provide a larger amount of sugars, and other microorganism options that contribute to improving ethanol/sugar yield in fermentation. This would increase the concentration of ethanol in the fermenter effluent and reduce energy costs in purification. For this purpose, it is proposed to set an ethanol concentration that reduces the energy requirements in distillation and improves the profitability of the process. Once known, it is possible to determine the sugars concentration that the feedstock must have to produce a desired ethanol concentration.

References

1. Liguori R and Faraco V, Biological processes for advancing lignocellulosic waste biorefinery by advocating circular economy. *Bioresour Technol* **215**:13–20 (2016).
2. Sherwood J, The significance of biomass in a circular economy. *Bioresour Technol* **300**(1–8):122755 (2020).
3. IATA, Annual Review (2018). Available: https://www.iata.org/contentassets/c81222d96c9a4e0bb4ff6ced0126f0bb/iata-annual-review-2018.pdf [19 March 2020].
4. Wei H, Liu W, Chen X, Yang Q, Li J and Chen H, Renewable bio-jet fuel production for aviation: A review. *Fuel* **254**:1–16 (2019).
5. IATA, Annual Review (2020). Available: https://www.iata.org/contentassets/c81222d96c9a4e0bb4ff6ced0126f0bb/iata-annual-review-2020.pdf [18 April 2021].

6. Graver B, Zhang K and Rutherford D, CO_2 Emissions from Commercial Aviation, 2018 (2019). Available: https://theicct.org/sites/default/files/publications/ICCT_CO2-commercl-aviation-2018_20190918.pdf [07 April 2020].
7. Ge M and Friedrich J, World Resources Institute. Available: https://www.wri.org/blog/2020/02/greenhouse-gas-emissions-by-country-sector [20 March 2020].
8. Ritchie H, Climate change and flying: What share of global CO2 emissions come from aviation? Available: https://ourworldindata.org/ [24 November 2020].
9. Cruz-Neves R, Colling-Klein B, da Silva RJ, Ferreira-Rezende MC, Funke A, Olivarez-Gómez E *et al*., A vision on biomass-to-liquids (BTL) thermochemical routes in integrated sugarcane biorefineries for biojet fuel production. *Rev Renew Sustain Energy* **119**:119 (2020).
10. Wang WC, Tao L, Marham J, Zhang Y, Tan E, Batan L *et al*., *Review of Biojet Fuel Conversion Technologies*. National Renewable Energy Laboratory, Denver (2016b).
11. Mawhood R, Gazis E, de Jong S, Hoefnagels R and Slade R, Production pathways for renewable jet fuel: A review of commercialization status and future prospects. *Biofuels Bioprod Biorefin* **10**:462–484 (2016).
12. Han GB, Jang JH, Ahn MH and Jung BH, Recent application of bio-alcohol: Bio-jet fuel, in *Alcohol Fuels. Current Technologies and Future Prospect*, ed. by Yun Y. IntechOpen, USA pp. 104–118 (2020).
13. Sankpal S and Naikwade P, Important bio-fuel crops: Advantages and disadvantages. *Int J Sci Eng Res* **4**:1–5 (2013).
14. Datta A, Hossain A and Roy S, An overview on biofuels and their advantages and disadvantages. *Asian J Chem* **31**:1851–1858 (2019).
15. Stankiewikcz A and Moulijn JA, Process intensification: Transforming chemical engineering. *Chem Eng Prog* **96**:22–34 (2000).
16. Yue D, You F and Snyder SW, Biomass-to-bioenergy and biofuel supply chain optimization: Overview, key issues and challenges. *Comput Chem Eng* **66**:36–56 (2014).
17. Faik A, Plant cell wall structure-pretreatment: The critical relationship in biomass conversion to fermentable sugars, in *Green Biomass Pretreatment for Biofuels Production*, ed. by Gu T. Springer, Ohio, pp. 1–30 (2013).
18. Bajpai P, *Developments in Bioethanol*. Springer, Kanpur (2018).
19. Geleynse S, Brandt K, Wolcott M, Garcia-Perez M and Zhang X, The alcohol-to-jet conversion pathway for drop-in biofuels: Techno-economic evaluation. *ChemSusChem* **11**:3728–3741 (2018).
20. Saavedra-Lopez J, Dagle RA, Dagle VL, Smith C and Albrecht KO, Oligomerization of ethanol-derived propene and isobutene mixtures to transportation fuels: Catalyst and process considerations. *Catal Sci Technol* **9**:1117–1131 (2019).
21. Santos CI, Silva CC, Mussatto SI, Osseweijer P, van der Wielen LAM and Posada JA, Integrated 1st and 2nd generation sugarcane bio-refinery for jet fuel production in Brazil: Techno-economic and greenhouse gas emissions assessment. *Renew Energy* **129**:733–747 (2018).
22. Kaltschmitt M and Neuling U eds, Alcohol-to-jet (AtJ), in *Biokerosene. Status and Prospects*. Springer, Berlin, pp. 543–574 (2018).
23. Kiss AA and Suszwalak DJ-PC, Enhanced bioethanol dehydration by extractive and azeotropic distillation in dividing-wall columns. *Sep Purif Technol* **86**:70–78 (2012).
24. Errico M and Rong BG, Synthesis of new separation processes for bioethanol production by extractive distillation. *Sep Purif Technol* **96**:58–67 (2012).
25. Ramírez-Márquez C, Segovia-Hernández JG, Hernández S, Errico M and Rong BG, Dynamic behavior of alternative separation processes for ethanol dehydration by extractive distillation. *Ind Eng Chem Res* **52**:17554–17561 (2013).
26. Bowling IM, Ponce-Ortega JM and El-Halwagi MM, Facility location and supply chain optimization for a biorefinery. *Ind Eng Chem Res* **50**(10):6276–6286 (2011).
27. Ng RTL and Maravelias C, Design of biofuel supply chains with variable regional depot and biorefinery locations. *Renew Energy* **100**:90–102 (2017).
28. Ng RTL and Maravelias C, Design of cellulosic ethanol supply chains with regional depots. *Ind Eng Chem Res* **2016**(55):3420–3432 (2016).
29. García-Serna J, Pérez-Barrigón L and Cocero MJ, New trends for design towards sustainability in chemical engineering: Green engineering. *Chem Eng J* **133**:7–30 (2007).
30. Foo DCY and El-Halwagi MM, *Process Intensification and Integration for Sustainable Design*, First edn. Wiley-VCH, Germany (2021).
31. SENER, Mapa de Ruta Tecnológica Bioturbosina (2017). Available: https://www.gob.mx/cms/uploads/attachment/file/324219/MRT_Bioturbosina_Final.pdf [07 April 2020].
32. SAGARPA (2015). Available: https://www.gob.mx/cms/uploads/attachment/file/346978/Manejo_de_residuos_Detallado.pdf. Accessed November 2022.
33. Sabiha-Hanim S and Abd Halim NA, Sugarcane bagasse pretreatment methods for ethanol production, in *Fuel Ethanol Production from Sugarcane*. IntechOpen, USA (2018).
34. Barros-Rios J, Romaní A, Garrote G and Ordas B, Biomass, sugar, and bioethanol potential of sweet corn. *GCB Bioenergy* **7**:153–160 (2014).
35. Hernández C, Escamilla-Alvarado C, Sánchez A, Alarcón E, Ziarelli F, Musele R *et al*., Wheat straw, corn stover, sugarcane, and agave biomasses: Chemical properties, availability, and cellulosic-bioethanol production potential in Mexico. *Biofuels Bioprod Biorefin* **13**:1143–1159 (2019).
36. Conde-Mejía C, Jiménez-Gutiérrez A and El-Halwagi M, A comparison of pretreatment methods for bioethanol production from lignocellulosic materials. *Process Saf Environ Prot* **90**:189–202 (2012).
37. Mokomele T, da Costa Sousa L, Balan V, van Rensburg E, Dale BE and Görgens JF, Ethanol production potential from AFEX™ and steam-exploded sugarcane residues for sugarcane biorefineries. *Biotechnol Biofuels* **11**:11 (2018).
38. Dagle RA, Wilkelman AD, Ramasamy KK, Lebarbier-Dagle V and Weber RS, Ethanol as a renewable building block for fuels and chemicals. *Ind Eng Chem Res* **59**:4843–4853 (2020).
39. Baldea M, Egdar TF, Stanley BL and Kiss AA, Modular manufacturing processes: Status, challenges and opportunities. *AIChE J* **63**:4262–4272 (2017).
40. Weber RS, Holladay JE, Jenks C, Panisko EA, Snowden-Swan LJ, Ramirez-Corredores M *et al*., Modularized production of fuels and other value-added products from distributed, wasted, or stranded feedstocks. *WIREs Energy Environ* **7**:1–18 (2018).
41. Gutiérrez-Antonio C, Romero-Izquierdo AG, Gómez-Castro FI and Hernández S, Supply chain for the production of biojet fuel, in *Production Processes of Renewable Aviation Fuel: Present Technologies and Future Trends*. Elsevier, The Netherland pp. 201–203 (2021).
42. Finkbeiner M, Pannok M, Fasel H, Riese J and Lier S, Modular production with bio-based resources in a decentral production network. *Chemie Ingenieur Technik* **2041-2045**:92 (2020).
43. Davis R, Tao L, Tan ECD, Biddy MJ, Beckham GT and Scarlata C, Process Design and Economics for the Conversion of

Lignocellulosic Biomass to Hydrocarbons: Dilute-Acid and Enzymatic Deconstruction of Biomass to Sugars and Biological Conversion of Sugars to Hydrocarbons. Technical Report, National Renewable Energy Laboratory (2013).
44. Santucci BS, Maziero P, Rabelo SC, Curvelo AAS and Pimienta MTB, Autohydrolysis of hemicelluloses from sugarcane bagasse during hydrothermal pretreatment: A kinetic assessment. *Bioenergy Res* **8**:1778–1787 (2015).
45. Liu ZH and Chen HZ, Xylose production from corn stover biomass by steam explosion combined with enzymatic digestibility. *Bioresour Technol* **193**:345–356 (2015).
46. Benjamin YCH and Görgens JF, Optimization of dilute sulfuric acid pretreatment to maximize combined sugar yield from sugarcane bagasse for ethanol production. *Appl Biochem Biotechnol* **172**:610–630 (2013).
47. Bondesson PM, Galbe M and Zacchi G, Ethanol and biogas production after steam pretreatment of corn stover with or without the addition of sulphuric acid. *Biotechnol Biofuels* **6**:1–11 (2013).
48. Zhu Y, Lee YY and Elander R, Optimization of dilute-acid pretreatment of corn stover using a high-solids percolation reactor. *Appl Biochem Biotechnol* **124**:1045–1054 (2005).
49. Souza-Aguiar R, Luciano-Silveira MR, Pitarelo AP, Corazza ML and Pereira-Ramos L, Kinetics of enzyme-catalyzed hydrolysis of steam-exploded sugarcane bagasse. *Bioresour Technol* **147**:416–423 (2013).
50. Kou X, Yang R, Zhao J, Lu J and Liu Y, Enzymatic saccharification and L-lactic acid fermentation of corn stover pretreated with liquid hot water by *Rhizopus oryzae*. *Bioresources* **8**:4899–4911 (2013).
51. An-Tran TT, Phung-Le TK, Mai PT and Nguyen DQ, Bioethanol production from lignocellulosic biomass, in *Alcohol Fuels*, ed. by Yun Y. IntechOpen, The Netherland pp. 507–520 (2019).
52. Lin Y, Zhang W, Li C, Sakakibara K, Tanaka S and Kong H, Factors affecting ethanol fermentation using *Saccharomyces cerevisiae* BY4742. *Biomass Bioenergy* **47**:395–401 (2012).
53. Conde-Mejía C, Jiménez-Gutiérrez A and Gómez-Castro FI, Dehydration, purification of bioethanol from a fermentation process: Alternatives for dehydration. *Comput Aided Chem Eng* **38**:373–378 (2016).
54. Kiss AA and Ignat RM, Innovative single step bioethanol dehydration in an extractive dividing-wall column. *Sep Purif Technol* **98**:290–297 (2012).
55. Errico M, Sanchez-Ramirez E, Quiroz-Ramìrez JJ, Segovia-Hernandez JG and Rong BG, Synthesis and design of new hybrid configurations for biobutanol purification. *Comput Chem Eng* **84**:482–492 (2016).
56. Petlyuk FB, Platonov VM and Slavinskii DM, Thermodynamically optimal method for separating multicomponent mixtures. *Int Chem Eng* **5**:555–561 (1965).
57. Yildirim Ö, Kiss AA and Kenig EY, Dividing wall columns in chemical process industry: A review on current activities. *Sep Purif Technol* **80**(3):403–417 (2011).
58. Byogy Renewables, Technical Memorandum for Analysis of Biofuels from Byogy Renewables. Memorandum. Department of the Air Force USA (2011).
59. Romero-García AG, Prado-Rubio OA, Contreras-Zarazúa G, Ramírez-Márquez C, Ramírez-Prado JH and Segovia-Hernández JG, Simultaneous design and controllability optimization for the reaction zone for furfural bioproduction. *Ind Eng Chem Res* **59**:15990–16003 (2020).
60. Contreras-Zarazúa G, Sánchez-Ramírez E, Vázquez-Castillo JA, Ponce-Ortega JM, Errico M, Kiss AA *et al*., Inherently safer design and optimization of intensified separation processes for furfural production. *Ind Eng Chem Res* **58**:6105–6120 (2019).
61. Sánchez-Ramírez E, Quiroz-Ramírez JJ, Segovia-Hernández JG, Hernández S and Ponce-Ortega JM, Economic and environmental optimization of the biobutanol purification process. *Clean Technol Environ Policy* **18**:395–411 (2016).
62. Quiroz-Ramírez JJ, Sánchez-Ramírez E, Segovia-Hernández JG, Hernández S and Ponce-Ortega JM, Optimal selection of feedstock for biobutanol production considering economic and environmental aspects. *Sustain Chem Eng* **5**:4018–4030 (2017).
63. López-Maldonado LA, Ponce-Ortega JM and Segovia-Hernández JG, Multiobjective synthesis of heat exchanger networks minimizing the total annual cost and the environmental impact. *Appl Therm Eng* **31**:1099–1113 (2011).
64. Goedkoop M and Spriensma R, *The Eco-Indicator 99. A Damage Oriented for Life Cycle Impact Assessment. Methodology Report and Manual for Designers*. PRé Consultants, Amersfoort (2001).
65. Alcocer-García H, Segovia-Hernández JG, Prado-Rubio OA, Sánchez-Ramírez E and Quiroz-Ramírez JJ, Multi-objective optimization of intensified processes for the purification of levulinic acid involving economic and environmental objectives. *Chem Eng Process Process Intensif* **136**:123–137 (2019).
66. Srinivas M and Rangaiah GP, Differential evolution with Tabu list for global optimization and its application to phase equilibrium and parameter estimation problems. *Ind Eng Chem Res* **46**:3410–3421 (2007).
67. Bonilla-Petriciolet A, Rangaiah GP and Segovia-Hernández JG, Evaluation of stochastic global optimization methods for modeling vapor–liquid equilibrium data. *Fluid Phase Equilibria* **287**:111–125 (2010).
68. Bonilla-Petriciolet A, Rangaiah GP and Segovia-Hernández JG, Constrained and unconstrained Gibbs free energy minimization in reactive systems using genetic algorithm and differential evolution with Tabu list. *Fluid Phase Equilibria* **300**:120–134 (2011).
69. Sánchez-Ramírez E, Quiroz-Ramírez JJ, Ramírez-Márquez C, Contreras-Zarazúa G, Segovia-Hernández JG and Bonilla-Petriciolet A, Optimization of intensified separation processes using differential evolution with Tabu list, in *Differential Evolution in Chemical Engineering. Developments and Applications*, Vol. **6**, ed. by Rangaiah PG and Sharma S. World Scientific, USA pp. 260–288 (2017).
70. Salas-Aguilar CL, Bonilla-Petriciolet A and Jaime-Leal JE, Optimización multi-objetivo del desempeño y consumo energético de procesos de destilación intensificados para sistemas cuaternarios. *Afinidad Revista de química teórica y aplicada* **75**:119–130 (2018).
71. Sánchez-Ramírez E, Quiroz-Ramírez JJ and Segovia-Hernández JG, Synthesis, design and optimization of schemes to produce 2,3-butanediol considering economic, environmental and safety issues, in *Proceedings of the 29th European Symposium on Computer Aided Process Engineering*, ed. by Kiss AA, Lakerveld R and Öskan L. Elsevier, Eindhoven (2019).
72. Vázquez-Castillo JA, Contreras-Zarazúa G, Segovia-Hernández JG and Kiss AA, Optimally designed reactive distillation processes for eco-efficient production of ethyl levulinate. *J Chem Technol Biotechnol* **94**:2131–2140 (2019).
73. Contreras-Zarazúa G, Vázquez-Castillo JA, Ramírez-Márquez C, Segovia-Hernández JG and Alcántara-Ávila JR, Multi-objective optimization involving cost and control properties in

reactive distillation processes to produce diphenyl carbonate. *Comput Chem Eng* **105**:185–196 (2017).
74. Ramírez-Márquez C, Contreras-Zarazúa G, Martín M and Segovia-Hernández JG, Safety, economic, and environmental optimization applied to three processes for the production of solar-grade silicon. *Sustain Chem Eng* **7**:5355–5366 (2019).
75. Segovia-Hernández JG and Gómez-Castro FI, *Stochastic Process Optimization Using Aspen Plus*®. CRC Press, USA (2017).
76. El-Halwagi AM, Rosas C, Ponce-Ortega JM, Jimenez-Gutierrez A, Mannan MS and El-Halwagi MM, Multiobjective optimization of biorefineries with economic and safety objectives. *AIChE J* **59**:2427–2434 (2013).
77. Santibañez-Aguilar JE, Gonzalez-Campos JB, Ponce-Ortega JM, Serna-Gonzalez M and El-Halwagi MM, Optimal planning and site selection for distributed multiproduct biorefineries involving economic, environmental and social objectives. *J Clean Prod* **65**:270–294 (2014).
78. Mota CJA, Peres-Pinto B and De-Lima AL, *Glycerol. A Versatile Renewable Feedstock for the Chemical Industry*. Springer, Germany (2017).
79. Towler G and Sinnott R, *Chemical Engineering Design. Principles, Practices and Economics of Plant and Process Design*. Elsevier, The Netherland (2012).
80. Ulrich GD and Vasudevan PT, How to estimate utility costs. *Chem Eng* **4**:66–69 (2006).
81. Argus, North America Sulfur and Sulfur Acid. Available: https://www.argusmedia.com/. Accessed November 2022.
82. EIA, Electric Power Monthly. Available: https://www.eia.gov/electricity/monthly/epm_table_grapher.php?t=epmt_5_03. Accessed November 2022.
83. Contreras-Zarazúa G, Martin-Martin M, Sánchez-Ramírez E and Segovia-Hernández JG, Furfural production from agricultural residues using different intensified separation and pretreatment alternatives. Economic and environmental assessment. *Chem Eng Process Process Intensifi* **171**:108569 (2021).
84. Statista, Average Monthly Industrial Water and Sewer Rates in the U.S. from 2001 to 2013 (in 1,000 U.S. dollars). https://www.statista.com/statistics/754676/average-us-industrial-water-and-sewage-costs. Accessed November 2022.
85. Wang L, Littlewood J and Murphy RJ, An economic and environmental evaluation for bamboo-derived bioethanol. *RSC Adv* **4**:29604–29611 (2014).

Raul Mauricio Rivas-Interian

Raul Mauricio Rivas-Interian obtained his bachelor's degree in industrial chemical engineering from the Autonomous University of Yucatan, Mexico, in 2017. He obtained his master's degree in chemical engineering (process integration) from the University of Guanajuato, Mexico, in 2021. His work has been focused on bioprocesses, mass transfer in bubble column bioreactors, biorefinery design, process intensification, and stochastic optimization.

Eduardo Sanchez-Ramirez

Eduardo Sánchez-Ramírez has been a professor in the Department of Chemical Engineering at the University of Guanajuato since 2017. He currently serves as academic coordinator of the bachelor's degree in chemical engineering. He has gained considerable experience in the areas of synthesis, design, simulation, control and optimization of chemical processes. His published contributions focus on the production of biofuels and base chemicals in the chemical industry. He received a PhD Summa Cum Laude in March, 2017.

Juan José Quiroz-Ramírez

Juan José Quiroz-Ramirez is currently the professor in the Department of Industrial Processes and Energy at CIATEC AC, Mexico. He obtained his PhD from the University of Guanajuato. His areas of interest include biofuels, process synthesis and design, process intensification, bio-based chemical blocks, and conversion of liquid wastes to fuels.

Juan Gabriel Segovia-Hernandez

Professor Juan Gabriel Segovia-Hernandez, is a professor in the Department of Chemical Engineering at the University of Guanajuato, Mexico, and has strong expertise in the synthesis, design, and optimization of (bio)processes. He has contributed to defining systematic methodologies to produce optimum sustainable and green processes for the production of several commodities. He also applied his methodologies to the production of biofuels and bio-based building blocks.

Appendix

A1 Impact factors for Ecoindicator-99 calculation

Table A1 shows the unit prices for the supplies used in this work to calculate total annual cost.

Table A1. Unit prices of supplies.

Supply	Unit price	Source
HP steam	0.048 \$ kg^{-1}	79
MP steam	0.039 \$ kg^{-1}	79
LP steam	0.027 \$ kg^{-1}	79
Cooling water	0.135 \$ ton^{-1}	80
Process water	1.19 \$ ton^{-1}	81
Electricity	0.0681 \$ kWh^{-1}	82
Sugarcane bagasse	25 \$ ton^{-1}	83
Corn stover	58.5 \$ ton^{-1}	83
Sulfuric acid	117.80 \$ ton^{-1}	84
Enzyme	507.0 \$ ton^{-1}	85
Glycerol	0.755 \$ ton^{-1}	78

A2 Impact factors for Ecoindicator-99 calculation

Table A2 shows the weight factors of the impact categories for electricity, steam, steel, and water used in this work.

Table A2. Weight factors of impact categories to measure Ecoindicador-99.[64]

Impact category	Electricity (points kWh^{-1})	Steam (points kg^{-1})	Steal (points kg^{-1})	Water (points kg^{-1})
Carcinogenic	1.290E–03	1.040E–04	6.320E–03	2.870E–06
Organic compounds	1.010E–05	1.560E–03	8.010E–02	1.320E–05
Climate change	4.070E–03	1.270E–03	1.310E–02	4.350E–06
Radiation	8.940E–05	1.910E–06	4.510E–04	4.170E–06
Ozone depletion	5.410E–07	7.780E–07	4.550E–06	1.630E–08
Ecotoxicity	2.140E–04	2.850E–04	7.450E–02	1.800E–06
Acidification	9.880E–04	1.210E–04	2.710E–03	9.520E–07
Land occupation	4.640E–04	8.600E–05	3.730E–03	1.700E–06
Mineral extraction	5.850E–05	8.870E–06	7.420E–02	1.270E–06
Fossil fuels	1.010E–02	1.240E–02	5.930E–02	1.550E–05